Journal of Cell Science

from the wound margin. Therefore, HB-EGF expression induced by wounding might itself stimulate further expression of HB-EGF at the leading edge via an autocrine loop. Fig. 6F shows a schematic illustration of our proposed skin wound healing mechanism. After injury, keratinocytes at the wound margin begin to express HB-EGF and migrate toward the wound site without proliferating. Next, the focal release of HB-EGF may trigger the migration of additional cells, rather than cell proliferation at the leading edge. Therefore, we conclude that HB-EGF is rapidly induced after injury and plays an important role in wound healing by up-regulating keratinocyte migration.

Nuclear transcription factors play important roles in almost all biological events resulting from growth factor signaling, and several nuclear transcription factors are thought to be involved in skin wound healing. Several mouse models with gene-targeted disruption of nuclear transcriptional factors have been analyzed for skin wound healing. Sano et al. (Sano et al., 1999) reported severe retardation of wound healing in keratinocyte-specific STAT3 knockout mice. D'Souza et al. (D'Souza et al., 2002) reported impaired skin wound healing in E2F-1 knockout mice. Recently, the development of keratinocyte-specific c-jun knockout mice was reported (Li et al., 2003; Zenz et al., 2003). These mice showed retarded wound healing, and the activation of EGFR was greatly decreased (Li et al., 2003). Since EGF itself is not produced by keratinocytes, the autocrine loop consisting of HB-EGF, EGFR and c-jun might be one of the major regulatory signal transduction mechanisms in skin wound healing.

In conclusion, HB-EGF is an important growth factor in epithelialization during skin wound healing in vivo, and acts mainly by stimulating migration, rather than proliferation, of keratinocytes.

This study was supported in part by grants from the Ministry of Education, Culture, Sport, Science and Technology of Japan (to Y.S., K.H., E.M., S.H.), the Ministry of Health, Labor, and Welfare of Japan (K.H.) and the Lydia O'Leary Memorial Foundation.

References

Coffey, R. J., Jr, Derynck, R., Wilcox, J. N., Bringman, T. S., Goustin, A. S., Moses, H. L. and Pittelkow, M. R. (1987). Production and auto-induction of transforming growth factor-alpha in human keratinocytes. *Nature* **328**, 817-820.

Cook, P. W., Mattox, P. A., Keeble, W. W., Pittelkow, M. R., Plowman, G. D., Shoyab, M., Adelman, J. P. and Shipley, G. D. (1991). A heparin sulfate-regulated human keratinocyte autocrine factor is similar or identical to amphiregulin. *Mol. Cell. Biol.* **11**, 2547-2557.

Cribbs, R. K., Luquette, M. H. and Besner, G. E. (1998). Acceleration of partial-thickness burn wound healing with topical application of heparin-binding EGF-like growth factor (HB-EGF). *J. Burn Care Rehabil.* **19**, 95-101.

Cribbs, R. K., Harding, P. A., Luquette, M. H. and Besner, G. E. (2002). Endogenous production of heparin-binding EGF-like growth factor during murine partial-thickness burn wound healing. *J. Burn Care Rehabil.* **23**, 116-125.

D'Souza, S. J., Vespa, A., Murkherjee, S., Maher, A., Pajak, A. and Dagnino, L. (2002). E2F-1 is essential for normal epidermal wound repair. *J. Biol. Chem.* **277**, 10626-10632.

Erickson, S. L., O'Shea, K. S., Ghaboosi, N., Loverro, L., Frantz, G., Bauer, M., Lu, L. H. and Moore, M. W. (1997). ErbB3 is required for normal cerebellar and cardiac development: a comparison with ErbB2-and heregulin-deficient mice. *Development* **124**, 4999-5011.

Falls, D. L. (2003). Neuregulins: functions, forms, and signaling strategies. *Exp. Cell Res.* **284**, 14-30.

Gassmann, M., Casagranda, F., Orioli, D., Simon, H., Lai, C., Klein, R. and Lemke, G. (1995). Aberrant neural and cardiac development in mice lacking the ErbB4 neuregulin receptor. *Nature* **378**, 390-394.

Grose, R. and Werner, S. (2003). Wound healing studies in transgenic and knockout mice. A review. *Methods Mol. Med.* **78**, 191-216.

Harari, D., Tzahar, E., Romano, J., Shelly, M., Pierce, J. H., Andrews, G. C. and Yarden, Y. (1999). Neuregulin-4: a novel growth factor that acts through the ErbB-4 receptor tyrosine kinase. *Oncogene* **18**, 2681-2689.

Hashimoto, K. (2000). Regulation of keratinocyte function by growth factors. *J. Dermatol. Sci.* **24**, S46-S50.

Hashimoto, K., Higashiyama, S., Asada, H., Hashimura, E., Kobayashi, T., Sudo, K., Nakagawa, T., Damm, D., Yoshikawa, K. and Taniguchi, N. (1994). Heparin-binding epidermal growth factor-like growth factor is an autocrine growth factor for human keratinocytes. *J. Biol. Chem.* **269**, 20060-20066.

Iwamoto, R., Yamazaki, S., Asakura, M., Takashima, S., Hasuwa, H., Miyado, K., Adachi, S., Kitakaze, M., Hashimoto, K., Raab, G. et al. (2003). Heparin-binding EGF-like growth factor and ErbB signaling is essential for heart function. *Proc. Natl. Acad. Sci. USA* **100**, 3221-3226.

Jorissen, R. N., Walker, F., Pouliot, N., Garrett, T. P., Ward, C. W. and Burgess, A. W. (2003). Epidermal growth factor receptor: mechanisms of activation and signalling. *Exp. Cell Res.* **284**, 31-53.

Lee, K. F., Simon, H., Chen, H., Bates, B., Hung, M. C. and Hauser, C. (1995). Requirement for neuregulin receptor erbB2 in neural and cardiac development. *Nature* **378**, 394-398.

Li, G., Gustafson-Brown, C., Hanks, S. K., Nason, K., Arbeit, J. M., Pogliano, K., Wisdom, R. M. and Johnson, R. S. (2003). c-Jun is essential for organization of the epidermal leading edge. *Dev. Cell* **4**, 865-877.

Luetteke, N. C., Qiu, T. H., Peiffer, R. L., Oliver, P., Smithies, O. and Lee, D. C. (1993). TGF alpha deficiency results in hair follicle and eye abnormalities in targeted and waved-1 mice. *Cell* **73**, 263-278.

Luetteke, N. C., Qiu, T. H., Fenton, S. E., Troyer, K. L., Riedel, R. F., Chang, A. and Lee, D. C. (1999). Targeted inactivation of the EGF and amphiregulin genes reveals distinct roles for EGF receptor ligands in mouse mammary gland development. *Development* **126**, 2739-2750.

Mann, G. B., Fowler, K. J., Gabriel, A., Nice, E. C., Williams, R. L. and Dunn, A. R. (1993). Mice with a null mutation of the TGF alpha gene have abnormal skin architecture, wavy hair, and curly whiskers and often develop corneal inflammation. *Cell* **73**, 249-261.

Marikovsky, M., Breuing, K., Liu, P. Y., Eriksson, E., Higashiyama, S., Farber, P., Abraham, J. and Klagsbrun, M. (1993). Appearance of heparin-binding EGF-like growth factor in wound fluid as a response to injury. *Proc. Natl. Acad. Sci. USA* **90**, 3889-3893.

McCarthy, D. W., Downing, M. T., Brigstock, D. R., Luquette, M. H., Brown, K. D., Abad, M. S. and Besner, G. E. (1996). Production of heparin-binding epidermal growth factor-like growth factor (HB-EGF) at sites of thermal injury in pediatric patients. *J. Invest. Dermatol.* **106**, 49-56.

Meyer, D. and Birchmeier, C. (1995). Multiple essential functions of neuregulin in development. *Nature* **378**, 386-390.

Miettinen, P. J., Berger, J. E., Meneses, J., Phung, Y., Pedersen, R. A., Werb, Z. and Derynck, R. (1995). Epithelial immaturity and multiorgan failure in mice lacking epidermal growth factor receptor. *Nature* **376**, 337-341.

Murillas, R., Larcher, F., Conti, C. J., Santos, M., Ullrich, A. and Jorcano, J. L. (1995). Expression of a dominant negative mutant of epidermal growth factor receptor in the epidermis of transgenic mice elicits striking alterations in hair follicle development and skin structure. *EMBO J.* **14**, 5216-5223.

Riethmacher, D., Sonnenberg-Riethmacher, E., Brinkmann, V., Yamaai, T., Lewin, G. R. and Birchmeier, C. (1997). Severe neuropathies in mice with targeted mutations in the ErbB3 receptor. *Nature* **389**, 725-730.

Sano, S., Itami, S., Takeda, K., Tarutani, M., Yamaguchi, Y., Miura, H., Yoshikawa, K., Akira, S. and Takeda, J. (1999). Keratinocyte-specific ablation of Stat3 exhibits impaired skin remodeling, but does not affect skin morphogenesis. *EMBO J.* **18**, 4657-4668.

Scheid, A., Meuli, M., Gassmann, M. and Wenger, R. H. (2000). Genetically modified mouse models in studies on cutaneous wound healing. *Exp. Physiol.* **85**, 687-704.

Shirakata, Y., Komurasaki, T., Toyoda, H., Hanakawa, Y., Yamasaki, K., Tokumaru, S., Sayama, K. and Hashimoto, K. (2000). Epiregulin, a novel member of the epidermal growth factor family, is an autocrine growth factor in normal human keratinocytes. *J. Biol. Chem.* **275**, 5748-5753.

Shirakata, Y., Tokumaru, S., Yamasaki, K., Sayama, K. and Hashimoto, K. (2003). So-called biological dressing effects of cultured epidermal sheets

are mediated by the production of EGF family, TGF-beta and VEGF. *J. Dermatol. Sci.* **32**, 209-215.

Sibilia, M. and Wagner, E. F. (1995). Strain-dependent epithelial defects in mice lacking the EGF receptor. *Science* **269**, 234-238.

Singer, A. J. and Clark, R. A. (1999). Cutaneous wound healing. *New Engl. J. Med.* **341**, 738-746.

Stoll, S., Garner, W. and Elder, J. (1997). Heparin-binding ligands mediate autocrine epidermal growth factor receptor activation In skin organ culture. *J. Clin. Invest.* **100**, 1271-1281.

Takeda, J., Sano, S., Tarutani, M., Umeda, J. and Kondoh, G. (2000). Conditional gene targeting and its application in the skin. *J. Dermatol. Sci.* **23**, 147-154.

Tokumaru, S., Higashiyama, S., Endo, T., Nakagawa, T., Miyagawa, J. I., Yamamori, K., Hanakawa, Y., Ohmoto, H., Yoshino, K., Shirakata, Y. et al. (2000). Ectodomain shedding of epidermal growth factor receptor ligands is required for keratinocyte migration in cutaneous wound healing. *J. Cell Biol.* **151**, 209-220.

Werner, S. and Grose, R. (2003). Regulation of wound healing by growth factors and cytokines. *Physiol. Rev.* **83**, 835-870.

Zenz, R., Scheuch, H., Martin, P., Frank, C., Eferl, R., Kenner, L., Sibilia, M. and Wagner, E. F. (2003). c-Jun regulates eyelid closure and skin tumor development through EGFR signaling. *Dev. Cell.* **4**, 879-889.

Journal of Cell Science

Available online at www.sciencedirect.com
SCIENCE DIRECT®
Biochemical and Biophysical Research Communications 335 (2005) 505–511
BBRC
www.elsevier.com/locate/ybbrc

dsRNA-mediated innate immunity of epidermal keratinocytes

Mikiko Tohyama [a], Xiuju Dai [a], Koji Sayama [a,*], Kenshi Yamasaki [a], Yuji Shirakata [a], Yasushi Hanakawa [a], Sho Tokumaru [a], Yoko Yahata [a], Lujun Yang [a], Hiroshi Nagai [a], Akira Takashima [b], Koji Hashimoto [a]

[a] *Department of Dermatology, Ehime University School of Medicine, Shitsukawa, Toon-city, Ehime 791-0295, Japan*
[b] *Department of Dermatology, University of Texas Medical School, Dallas, TX 75390, USA*

Received 15 July 2005

Abstract

MIP-1α, a CC chemokine, recruits monocytes, natural killer cells, lymphocytes, and neutrophils, and plays a critical role in viral infection. Since, the lesional epidermis of herpes zoster expressed MIP-1α, we hypothesized that keratinocytes produce MIP-1α in response to virus-associated dsRNA via TLR3. To investigate this, we examined cultured human keratinocytes for MIP-1α production induced by poly(I:C), a TLR3 ligand. Poly(I:C) treatment induced MIP-1α production, interestingly, poly(I:C)-induced IFN-α and -β production preceded MIP-1α production. A neutralizing antibody for IFN-β significantly inhibited the poly(I:C)-induced MIP-1α production indicating that MIP-1α production is via IFN-β. IFN-α priming enhanced TLR3 expression and MIP-1α production in poly(I:C)-treated keratinocytes. This suggests that IFN-α enhanced the TLR3 expression and reinforced the response of keratinocytes to poly(I:C), which resulted in an increase in MIP-1α production. In conclusion, normal human keratinocytes produce MIP-1α in response to dsRNA via TLR3, and this production is regulated by IFN-α/β.
© 2005 Elsevier Inc. All rights reserved.

Keywords: Viral infection; IFN-α; IFN-β; MIP-1α; Herpes virus; Skin; Keratinocyte

The innate immune mechanism is characterized by its rapid and undiversified response, in contrast to the adaptive immune response of T and B lymphocytes. The cells and organs that contact microbial pathogens play direct roles in innate immunity. The functions of lymphocytes, macrophages, neutrophils, and dendritic cells in innate immunity have been well characterized [1]. In contrast, the role of keratinocytes in innate immunity is poorly understood, although keratinocytes form the epidermis, the body's first line of defense against invading microbial pathogens.

The herpes simplex virus (HSV) and varicella-zoster virus (VZV) cause common infections of the skin. These viruses proliferate in the epidermal keratinocytes after infection, resulting in ballooning degeneration of the epidermal keratinocytes and vesicle formation. The innate immune response, including immediate interferon (IFN) production and cellular response, plays a critical role in defense during both primary and recurrent infection. IFN-α/β is produced by infected cells within hours following infection and reduces herpes virus replication [2]. IFN-α/β prepares the cells neighboring infected cells to enter an antiviral state [3]. Neutrophils, macrophages, and natural killer (NK) cell infiltration appear immediately in the skin of the lesion [4]. Neutrophils are the first and predominant cells appearing in herpes lesions and comprise a nonspecific antiviral defense [5]. Macrophages have phagocytic activity and are significant sources of inflammatory cytokines including IFN-α/β and TNF-α, and the antiviral compound nitric oxide [4]. The recruitment of NK cells is a prerequisite for the innate immune response in viral infection [6].

* Corresponding author. Fax: +81 89 960 5352.
E-mail address: sayama@m.ehime-u.ac.jp (K. Sayama).

0006-291X/$ - see front matter. © 2005 Elsevier Inc. All rights reserved.
doi:10.1016/j.bbrc.2005.07.105

Although the infiltration and functions of these inflammatory cells have been studied, the mechanism by which these inflammatory cells are recruited into the skin lesion has not yet been clarified.

Chemokines play important roles in the infiltration of inflammatory cells. As epidermal keratinocytes produce many cytokines and chemokines, it seems likely that chemokines produced by the epidermal keratinocytes attract inflammatory cells into herpes virus-infected skin. In fact, several chemokines, including macrophage inflammatory protein 1 alpha (MIP-1α)/CCL3, MIP-1β/CCL4, and RANTES/CCL5, are found in the vesicle fluid of human recurrent herpes simplex lesions [7]. Among these chemokines, MIP-1α plays an important role in antiviral defense [8]. In MIP-1α-deficient mice, the infiltration of mononuclear cells, neutrophils, and eosinophils is reduced during viral infection [9]. MIP-1α is also involved in NK cell inflammation and NK cell migration in murine cytomegalovirus infection [10]. In vivo herpes virus-infected keratinocytes produce MIP-1α, however, uninfected keratinocytes do not produce MIP-1α upon stimulation with herpes simplex virus antigen, and keratinocytes treated with TNF-α, IL-1, or IFN-γ could not express MIP-1α [7]. Based on these observations, MIP-1α seems to be a key chemokine for mediating an innate immune response in viral infection.

Toll-like receptors (TLRs) are prominent among the initial triggers that allow the infected host to develop an immune response. Among the TLRs identified in human beings, TLR3 and TLR8 are thought to be important receptors in activating natural immune responses against viral infection [11]. These receptors recognize dsRNA and ssRNA, respectively, which are synthesized during viral replication, and they induce the expression of antiviral genes such as IFN-α/β. A dsRNA is produced in almost all viral infections, including that caused by herpes virus [12]. In epidermal keratinocytes, stimulation with dsRNA causes transcriptional expression of the IFN-α/β genes [13], which is proposedly mediated by TLR3 since epidermal keratinocytes express TLR3 mRNA [14]. However, no previous reports have investigated the mechanism of MIP-1α production in epidermal keratinocytes.

In this study, we report for the first time that epidermal keratinocytes produce MIP-1α dependent upon treatment with polyinosine:polycytidylic acid [poly(I:C)], a synthetic dsRNA, and a specific ligand for TLR3. We also demonstrated that poly(I:C)-dependent MIP-1α production is regulated by type I IFN.

Materials and methods

Materials and antibodies. IFN-α and IFN-β were gifts from Otsuka Pharmaceutical (Tokyo, Japan). Goat anti-MIP-1α, mouse monoclonal anti-IFN-α, and mouse monoclonal anti-IFN-β were purchased from R&D system (Minneapolis, MN, USA). Poly(I:C) (Amersham, Piscataway, NJ, USA) and poly(I) (Sigma–Aldrich, St. Louis, MO, USA) were used to stimulate keratinocytes.

Skin samples and immunohistochemical analysis. Biopsy specimens were obtained from freshly developed herpes zoster lesions of three patients after informed consent. Skin samples were fixed in 10% buffered formalin for conventional paraffin sections. MIP-1α expression was examined by a biotin-avidin method, according to the manufacturer's protocol (Histofine SAB-PO Kit, Nichirei, Tokyo, Japan). The sections were exposed to primary antibodies (1:100) for 1 h at 37 °C. Peroxidase detection was performed with 3-amino-9-ethylcarbazole as a chromogen. Finally, sections were counterstained with hematoxylin.

The study was conducted according to the Declaration of Helsinki Principles. All of the procedures that involved human subjects received prior approval from the Ethical Committee of Ehime University School of Medicine, and all the subjects provided written informed consent.

Keratinocyte cultures. Human skin samples were obtained after plastic surgery. Normal human skin was cut into strips 3–5 mm long and incubated overnight at 4 °C in Dulbecco's modified Eagle's medium containing 250 U/ml of dispase. After the separation of the epidermis from the dermis using forceps, the epidermal sheets were rinsed with PBS and incubated in a 0.25% trypsin solution for 10 min at 37 °C. Keratinocytes were rinsed, collected by centrifugation, and then resuspended in MCDB153 medium supplemented with insulin (5 μg/ml), hydrocortisone (0.5 μM), ethanolamine (0.1 mM), phosphoethanolamine (0.1 mM), and bovine hypothalamic extract (BHE; 50 μg/ml). Cells that had been passaged four times were used in the experiments as previously described.

RNA preparation, RT-PCR, and real-time PCR. Total RNA from cultured human keratinocytes and epidermal sheets was prepared using Isogen (Nippon Gene, Tokyo, Japan). The epidermal sheet was separated from the dermis by heat treatment (60 °C for 1 min). The RT-PCR was performed using RT-PCR High Plus (Toyobo, Osaka, Japan) as described previously [15]. In brief, cDNA was generated by reverse transcription of total RNA for 30 min at 60 °C and was then heated to 94 °C for 2 min. Thirty PCR cycles were used to amplify MIP-1α, 40 cycles for TLR3, and 25 cycles for GAPDH. The primers were: for MIP-1α, 5′-CACCATGGCTCTCTGCAAC-3′ and 5′-TATTTCTGGACCCACTCCTC-3′; for TLR3, 5′-GGAATTCGGAATCTGTCTCTGAGTA-3′ and 5′-CAAGCTTGAGTGAGGCAAGGGAAATAC-3′; and for GAPDH, 5′-ACCACAGTCCATGCCATCAC-3′ and 5′-TCCACCACCCTGTTGCTGTA-3′. The PCR products were visualized on 2% agarose gels containing ethidium bromide and were identified by size and direct DNA sequencing.

Real-time RT-PCR was performed in an ABI PRISM 7700 sequence detector (PE Applied Biosystems, NJ, USA). The primers and probes used for real-time PCR were purchased from Applied Biosystems (Norwalk, CT). RNA analysis was carried out using the TaqMan RT-PCR Master Mix reagents kit (Applied Biosystems). cDNA synthesis and PCRs were performed as described previously [15], according to the manufacturers' suggested protocols. The quantification of gene expression was performed using the comparative CT method as described previously [15]. The target gene expression in test samples was normalized to the corresponding GAPDH level and was reported as the fold difference relative to the GAPDH gene expression. In this study, each assay was performed in triplicate.

ELISAs. ELISA kits for IFN-α and MIP-1α were purchased from Endogen (Auburn, MA, USA), and the IFN-β ELISA kit was purchased from PBL Biomedical Laboratories (Tokyo, Japan). Optical density was measured with an Immuno Mini NJ-2300 microplate reader (Nalge Nunc International K.K., Tokyo, Japan). All assays were done in triplicate.

Statistical analyses. The data were collected from at least three independent experiments. Quantitative data are expressed as the means ± SE. Statistical significance was determined by a paired Student's *t* test. Differences were considered to be statistically significant

for $P < 0.05$. The levels of statistical significance are indicated in figures as follows: $*P < 0.05$; $**P < 0.01$; and $***P < 0.001$.

Results

Expression of MIP-1α in the epidermis of herpes zoster lesions

Skin lesions of herpes zoster are characterized by ballooning and reticular degeneration of the epidermal cells, infiltration of various inflammatory cells including PMN, and vasculitis in the upper dermis. Immunohistochemical analysis showed remarkable staining of MIP-1α in the epidermal keratinocytes (Fig. 1A) but not in the normal human epidermis (Fig. 1C). These data suggest that epidermal keratinocytes produce MIP-1α in response to viral infection.

MIP-1α production by poly(I:C)

To analyze whether keratinocytes react to virus-associated dsRNA, we next stimulated keratinocytes with poly(I:C), a synthetic dsRNA, and a specific ligand for TLR3. Poly(I:C) induced the expression of MIP-1α mRNA, which was detected at 8 h after stimulation with 100 ng/ml poly(I:C) and increased in a time-dependent manner (Fig. 2A). MIP-1α production was further confirmed by its protein expression in culture supernatants by ELISA. Treatment with poly(I:C) induced MIP-1α production in a dose-dependent manner (Fig. 2B), while

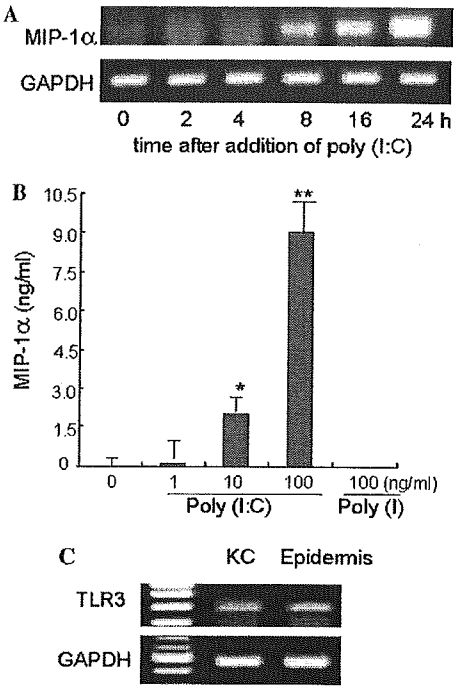

Fig. 2. Poly(I:C) induced MIP-1α production in keratinocytes. (A) Keratinocytes were stimulated with 100 ng/ml poly(I:C) for the time indicated. RT-PCR was performed to detect the expression of MIP-1α mRNA. The lower part of the panel shows GAPDH mRNA as a control. (B) Keratinocytes were stimulated with poly(I:C), poly(I) for 24 h, culture supernatants were collected, and ELISA was performed to detect the expression of the MIP-1α protein. (C) The expression of TLR3 was detected by RT-PCR in the cultured epidermal keratinocytes and epidermis.

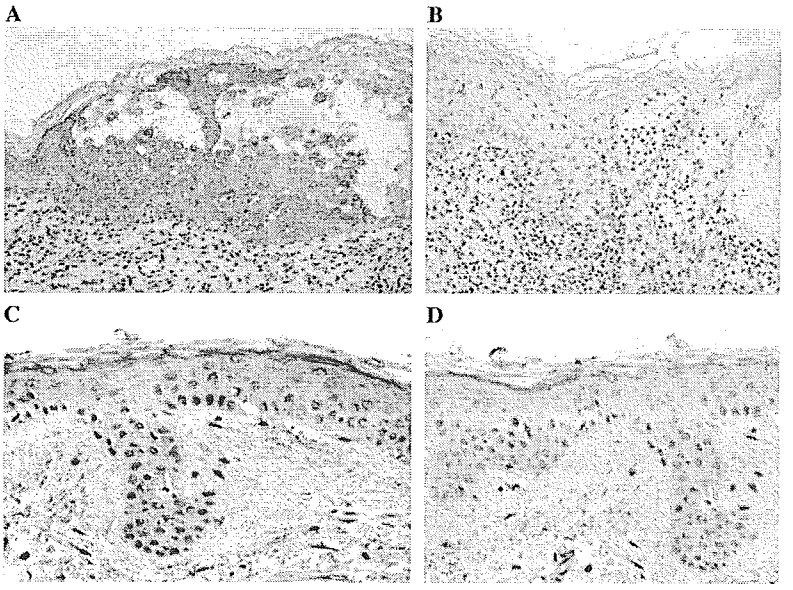

Fig. 1. Immunohistochemical analysis of MIP-1α in the skin of herpes zoster lesions. Lesional skin of herpes zoster (A,B) and normal human skin (C,D) were immunohistochemically stained with goat anti-MIP-1α (A,C) or control IgG (B,D). After staining, the sections were counterstained with hematoxylin.

the addition of polyinosine [poly(I)], a synthetic single-stranded RNA analogue, and a ligand for TLR8 not for TLR3, did not stimulate MIP-1α production in human keratinocytes. Although cytokines augment MIP-1α production in monocytes, colon epithelial cells, and fibroblasts [8], stimulation with single or a combination of cytokines, such as, TNF-α, IFN-γ, IL-1α, and IFN-α did not induce MIP-1α production in human keratinocytes (data not shown).

We next analyzed the expression of TLR3. As shown in Fig. 2C, both normal human epidermis and cultured normal human keratinocytes expressed TLR3 mRNA when analyzed by RT-PCR. These data suggest that MIP-1α production is dependent on the TLR3 signaling pathway.

Poly(I:C)-induced IFN-α/β production prior to MIP-1α production

Type I IFN plays important roles in viral infection. IFN-α and IFN-β are rapidly produced by infected cells during viral infection and reduce virus replication [2], they prepare neighboring cells to enter an antiviral state [3]. Poly(I:C) has been shown to stimulate the expression of IFN-α/β in human uterine epithelial cells [16]. We analyzed IFN-α/β mRNA expression in poly(I:C)-treated keratinocytes by real-time RT-PCR. As shown in Fig. 3A, IFN-β mRNA was rapidly induced, and its highest expression was found at 4 h after the addition of poly(I:C). IFN-α mRNA increased later than IFN-β, and the highest level of IFN-α mRNA was found at 8 h after treatment (Fig. 3A). Interestingly, the induction of MIP-1α mRNA by poly(I:C) occurred after the induction of IFN-β. MIP-1α mRNA was expressed from 4 h, and was increased in time-dependent manner (Fig. 3A). Next, we measured their protein expressions in the culture supernatants by ELISA. After addition of poly(I:C), IFN-α protein significantly increased from 12 h and peaked at 24 h, IFN-β production increased earlier and peaked at 12 h after stimulation, and significant MIP-1α protein was detected from 12 h and increased until 36 h (Fig. 3B). These data suggest a possible relationship between IFN-α/β and MIP-1α production in poly(I:C)-treated keratinocytes.

Regulation of MIP-1α production by IFN-β

In order to investigate whether IFN-α or -β was responsible for the production of MIP-1α, we treated keratinocytes with poly(I:C) in the presence or absence of anti-IFN-α/β polyclonal antibodies. Neutralization with anti-IFN-β antibody significantly reduced MIP-1α production induced by poly(I:C) (Fig. 4), while neutralization with anti-IFN-α antibody only showed slight effect on MIP-1α production. Therefore, IFN-β not IFN-α is an essential regulator for MIP-1α production in poly(I:C)-treated human keratinocytes.

Enhancement of poly(I:C)-induced MIP-1α production through increased TLR3 expression by priming with IFN-α/β

Although neutralizing IFN-α could not abolish poly(I:C)-induced MIP-1α production, priming with

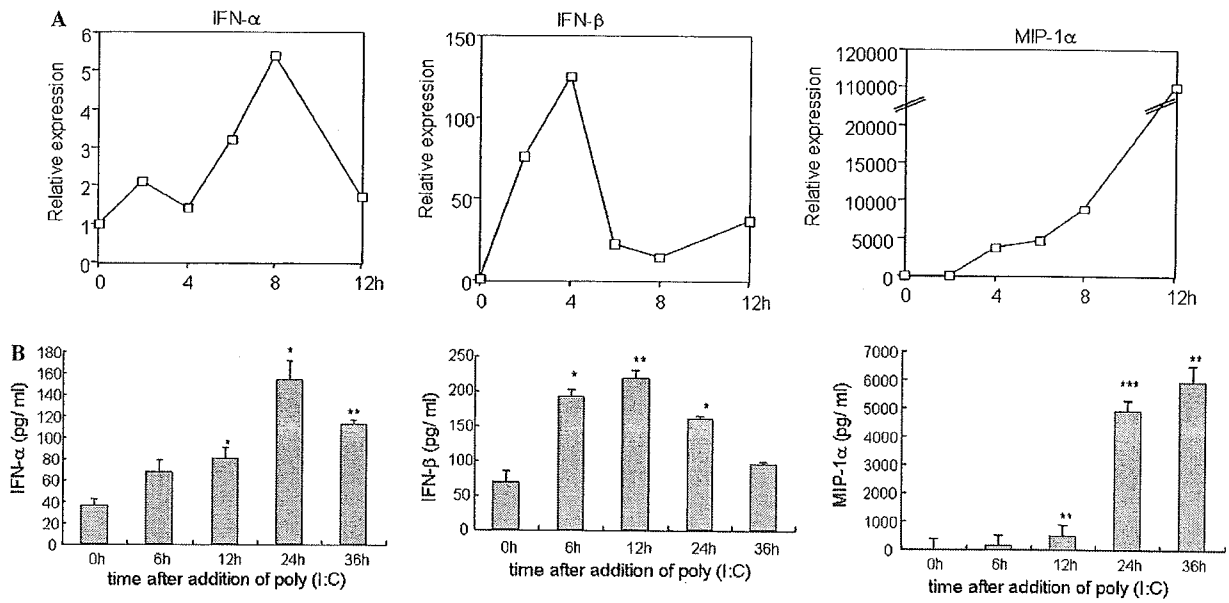

Fig. 3. Poly(I:C)-induced IFN-α/β production preceded MIP-1α production. (A) Keratinocytes were stimulated with 100 ng/ml poly(I:C) for the time indicated. RT-PCR was performed to detect the expression of IFN-α, IFN-β, and MIP-1α mRNA. (B) Keratinocytes were stimulated with 100 ng/ml poly(I:C) for the time indicated. ELISA was performed to determine the levels of IFN-α, IFN-β, and MIP-1α proteins.

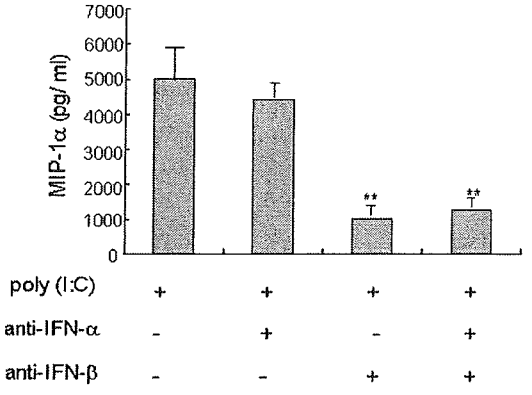

Fig. 4. Neutralizing IFN-β blocked poly(I:C)-induced MIP-1α production. The cultures were neutralized with anti-IFN-α antibody (5 μg/ml) or with anti-IFN-β antibody (5 μg/ml) for 1 h before stimulation with 100 ng/ml poly(I:C), cultures were incubated for another 24 h after addition of poly(I:C). Supernatants were analyzed by ELISA to detect MIP-1α production.

IFN-α strongly enhances poly(I:C)-induced MIP-1α induction in human keratinocytes (Fig. 5A), confirming the report in LPS-treated monocytes and fibroblasts [17]. MIP-1α production was enhanced about 3-fold by pretreatment with 100 U/ml IFN-α (Fig. 5A). A similar but weak effect was observed when keratinocytes were primed with IFN-β (Fig. 5A).

It was reported that IFN-α up-regulated the expression of TLR3 in macrophages, in A549 human lung carcinoma cells, and in human endothelial cells [18,19]. We speculated that increased TLR3 by IFN-α accounts for the enhancement of MIP-1α production in poly(I:C)-treated keratinocytes [19]. Treatment with 100 IU/ml IFN-α or with 100 IU/ml IFN-β increased TLR3 mRNA expression more than 8-fold compared with that of the control (Fig. 5B). These results suggest that the enhancement of poly(I:C)-induced MIP-1α production by priming with IFN-α/β may be attributable to increased TLR3 expression and amplified TLR3 signal.

Discussion

TLR3 plays a critical role in innate immunity to viral infections [11]. Almost all viruses, including DNA viruses, produce dsRNA [12]. Viral-associated dsRNA exists in infected cells and leaks from damaged cells. Neighboring cells are also affected by dsRNA. In the skin, keratinocytes are the primary target for viral infection. Infection with viruses such as HSV or VZV stimulates keratinocytes to produce dsRNA. Fig. 6 summarizes the results of dsRNA-provoked keratinocyte reaction: dsRNA enhances IFN-α/β production probably via TLR3, and TLR3 signaling also increases MIP-1α production. It is possible that dsRNA–TLR3 pathway first induces type I IFNs, then the produced type I IFNs activate the transcription of the MIP-1α gene in human keratinocytes, since MIP-1α is directly induced by type I IFNs [20] and neutralizing IFN-β signal blocks dsRNA-stimulated MIP-1α (Fig. 4). IFN-α and -β produced from the neighboring keratinocytes or from plasmacytoid dendritic cells also enhance TLR3 expression, which amplifies TLR3 signaling and results in the production of high amounts of MIP-1α. MIP-1α attracts NK cells, neutrophils, and various subsets of lymphocytes, and inhibits the expansion of viral infection in the skin. This is the first report describing MIP-1α production from keratinocytes caused by dsRNA via TLR3 and its regulation by IFN-α/β.

Viruses replicate and produce dsRNA in the cytoplasm before cell lysis occurs, and TLRs are a group of membrane proteins. This has led to the assumption that a viral sensor other than TLR3 must exist in the cytoplasm [21]. RNA helicase retinoic acid inducible gene (RIG-I) probably serves as this kind of cytoplasmic sensor, as RIG-I has been demonstrated to activate IRF-3 and to induce IFN-β production [21]. It has been reported that the responses to viral infection or to intracellular dsRNA were lessened in the absence of RIG-I, whereas extracellular dsRNA-stimulated responses mediated by TLR3 remained intact [22]. Both TLR3 and RIG-I sense the immune reaction to virus in vivo. It is

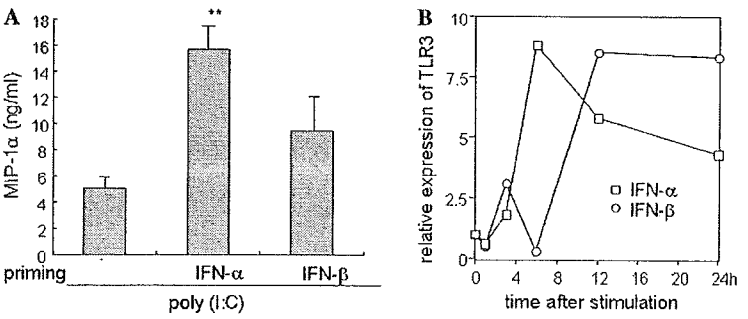

Fig. 5. IFN-α/β priming enhanced poly(I:C) induced MIP-1α production. (A) Keratinocytes were primed by 100 IU/ml IFN-α and IFN-β for 24 h, and treated with 100 ng/ml poly(I:C) for another 16 h after extensive washing with culture medium. Culture supernatants were obtained, and ELISA was performed to detect the level of MIP-1α. (B) Keratinocytes were stimulated with 100 IU/ml IFN-α or with 100 IU/ml IFN-β for the time indicated, total RNA was extracted, and RT-PCR was performed to determine the level of expression of TLR3 mRNA.

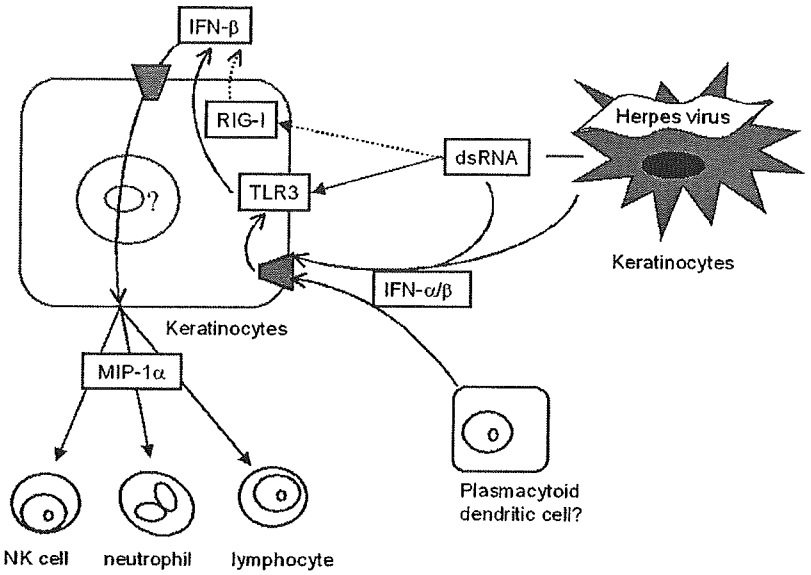

Fig. 6. Molecular mechanism of dsRNA-induced MIP-1α production in keratinocytes. This schema presents the possible mechanism of MIP-1α induction in response to viral infection in keratinocytes. After infection with virus or treatment with dsRNA, IFN-α/β is secreted by keratinocytes and MIP-1α is induced later. In turn, the produced IFN-α/β increases the expression of TLR3, which results in signal amplification. The induced IFN-β probably accounts for the induced MIP-1α expression in the viral infection of keratinocytes.

possible that MIP-1α production from keratinocytes induced by herpes virus infection is partially via RIG-I. Therefore, the involvement of RIG-I in the virally induced innate immune response of keratinocytes should be clarified in the future.

In the case of dsRNA-activated signals, the involvement of the dsRNA-dependent protein kinase PKR has also been suggested [23]. PKR exists in most cell types and trans-autophosphorylates in response to poly(I:C) treatment, to transduce the poly(I:C) signal. PKR has been shown to regulate poly(I:C)-induced TNFα [24]. However, PKR is not the kinase responsible for the activation of IRF-3 [23]. Furthermore, we did not detect the phosphorylation of PKR in poly(I:C)-treated keratinocytes (data not shown). All of these events support the suggestion that the poly(I:C)-stimulated signal in keratinocytes is independent of PKR.

IFNs are important proinflammatory cytokines, and IFN-α and -β induce or enhance an inflammatory reaction in response to viral infection [3]. After VZV infection, the expression of IFN-α is up-regulated in neighboring keratinocytes of the epidermis [25], and in the plasmacytoid dendritic cells of the dermis [26]. Poly(I:C) treatment stimulates keratinocytes to produce IFN-α/β (Fig. 3), confirmed the previous report in uterine epithelial cells [16]. And priming with IFN-α significantly enhanced poly(I:C)-induced MIP-1α production (Fig. 5), which is probably dependent on the increased sensitivity of keratinocytes to poly(I:C), as TLR3 expression is significantly increased by IFN-α priming in keratinocytes, which is consistent with the previous reports in epithelial, endothelial, macrophages and human lung carcinoma cells [18,19]. In this study, we found that IFN-β not IFN-α is essential for poly(I:C)-induced MIP-1α production, while priming with IFN-α not with IFN-β significantly increased MIP-1α induction though IFN-β also stimulated TLR3 expression as IFN-α did in human keratinocytes. Taken together, it is indicated that TLR3-mediated IFN-β expression initiate MIP-1α production in keratinocytes, and IFN-α amplifies TLR3 to further enhance MIP-1α production and strengthen the antiviral response [19]. Therefore, IFN-α from keratinocytes or plasmacytoid dendritic cells of skin lesion during viral infection may enhance the production of MIP-1α by amplifying TLR3 signal pathway.

In conclusion, normal human keratinocytes produce MIP-1α in response to dsRNA, and this MIP-1α production is regulated by IFN-α/β. Through MIP-1α production, keratinocytes recruit infiltrating cells and inhibit the expansion of viral infection in the skin.

Acknowledgment

We thank Teruko Tsuda and Eriko Tan for technical assistance.

References

[1] M.C. Carroll, C.A. Janeway, Curr. Opin. Immunol. 11 (1999) 11–12.

[2] L.E. Schnipper, M. Levin, C.S. Crumpacker, B.A. Gilchrest, J. Invest. Dermatol. 82 (1984) 94–96.
[3] C.E. Samuel, Clin. Microbiol. Rev. 14 (2001) 778–809, table of contents..
[4] R.J. Duerst, L.A. Morrison, Viral Immunol. 16 (2003) 475–490.
[5] D.A. Stevens, R.A. Ferrington, G.W. Jordan, T.C. Merigan, J. Infect. Dis. 131 (1975) 509–515.
[6] C.A. Biron, L. Brossay, Curr. Opin. Immunol. 13 (2001) 458–464.
[7] Z. Mikloska, V.A. Danis, S. Adams, A.R. Lloyd, D.L. Adrian, A.L. Cunningham, J. Infect. Dis. 177 (1998) 827–838.
[8] P. Menten, A. Wuyts, J. Van Damme, Cytokine Growth Factor Rev. 13 (2002) 455–481.
[9] D.N. Cook, M.A. Beck, T.M. Coffman, S.L. Kirby, J.F. Sheridan, I.B. Pragnell, O. Smithies, Science 269 (1995) 1583–1585.
[10] T.P. Salazar-Mather, J.S. Orange, C.A. Biron, J. Exp. Med. 187 (1998) 1–14.
[11] L. Alexopoulou, A.C. Holt, R. Medzhitov, R.A. Flavell, Nature 413 (2001) 732–738.
[12] J.A. Majde, J. Interferon Cytokine Res. 20 (2000) 259–272.
[13] H. Fujisawa, S. Kondo, B. Wang, G.M. Shivji, D.N. Sauder, J. Interferon Cytokine Res. 17 (1997) 721–725.
[14] M. Mempel, V. Voelcker, G. Kollisch, C. Plank, R. Rad, M. Gerhard, C. Schnopp, P. Fraunberger, A.K. Walli, J. Ring, D. Abeck, M. Ollert, J. Invest. Dermatol. 121 (2003) 1389–1396.
[15] X. Dai, K. Yamasaki, L. Yang, K. Sayama, Y. Shirakata, S. Tokumara, Y. Yahata, M. Tohyama, K. Hashimoto, J. Invest. Dermatol. 122 (2004) 1356–1364.
[16] T.M. Schaefer, J.V. Fahey, J.A. Wright, C.R. Wira, J. Immunol. 174 (2005) 992–1002.
[17] G. Bug, M.J. Aman, T. Tretter, C. Huber, C. Peschel, Exp. Hematol. 26 (1998) 117–123.
[18] M. Miettinen, T. Sareneva, I. Julkunen, S. Matikainen, Genes Immun. 2 (2001) 349–355.
[19] J. Tissari, J. Siren, S. Meri, I. Julkunen, S. Matikainen, J. Immunol. 174 (2005) 4289–4294.
[20] T.P. Salazar-Mather, C.A. Lewis, C.A. Biron, J. Clin. Invest. 110 (2002) 321–330.
[21] D.E. Levy, I.J. Marie, Nat. Immunol. 5 (2004) 699–701.
[22] M. Yoneyama, M. Kikuchi, T. Natsukawa, N. Shinobu, T. Imaizumi, M. Miyagishi, K. Taira, S. Akira, T. Fujita, Nat. Immunol. 5 (2004) 730–737.
[23] W.M. Chu, D. Ostertag, Z.W. Li, L. Chang, Y. Chen, Y. Hu, B. Williams, J. Perrault, M. Karin, Immunity 11 (1999) 721–731.
[24] T.R. Meusel, K.E. Kehoe, F. Imani, J. Immunol. 168 (2002) 6429–6435.
[25] C.C. Ku, L. Zerboni, H. Ito, B.S. Graham, M. Wallace, A.M. Arvin, J. Exp. Med. 200 (2004) 917–925.
[26] F.L. Jahnsen, L. Farkas, F. Lund-Johansen, P. Brandtzaeg, Hum. Immunol. 63 (2002) 1201–1205.

Induction of Keratinocyte Migration via Transactivation of the Epidermal Growth Factor Receptor by the Antimicrobial Peptide LL-37[1]

Sho Tokumaru,[2]* Koji Sayama,[2,3]* Yuji Shirakata,* Hitoshi Komatsuzawa,† Kazuhisa Ouhara,† Yasushi Hanakawa,* Yoko Yahata,* Xiuju Dai,* Mikiko Tohyama,* Hiroshi Nagai,* Lujun Yang,* Shigeki Higashiyama,‡ Akihiko Yoshimura,§ Motoyuki Sugai,† and Koji Hashimoto*

The closure of skin wounds is essential for resistance against microbial pathogens, and keratinocyte migration is an important step in skin wound healing. Cathelicidin hCAP18/LL-37 is an innate antimicrobial peptide that is expressed in the skin and acts to eliminate microbial pathogens. Because hCAP18/LL-37 is up-regulated at skin wound sites, we hypothesized that LL-37 induces keratinocyte migration. In this study, we found that 1 μg/ml LL-37 induced the maximum level of keratinocyte migration in the Boyden chamber assay. In addition, LL-37 phosphorylated the epidermal growth factor receptor (EGFR) after 10 min, which suggests that LL-37-induced keratinocyte migration occurs via EGFR transactivation. To test this assumption, we used inhibitors that block the sequential steps of EGFR transactivation, such as OSU8-1, CRM197, anti-EGFR no. 225 Ab, and AG1478. All of these inhibitors completely blocked LL-37-induced keratinocyte migration, which indicates that migration occurs via HB-EGF-mediated EGFR transactivation. Furthermore, CRM197, anti-EGFR no. 225, and AG1478 blocked the LL-37-induced phosphorylation of STAT3, and transfection with a dominant-negative mutant of STAT3 abolished LL-37-induced keratinocyte migration, indicating the involvement of the STAT3 pathway downstream of EGFR transactivation. Finally, we tested whether the suppressor of cytokine signaling (SOCS)/cytokine-inducible Src homology 2-containing protein (CIS) family of negative regulators of STAT3 regulates LL-37-induced keratinocyte migration. Transfection with SOCS1/Jak2 binding protein or SOCS3/CIS3 almost completely abolished LL-37-induced keratinocyte migration. In conclusion, LL-37 induces keratinocyte migration via heparin-binding-EGF-mediated transactivation of EGFR, and SOCS1/Jak 2 binding and SOCS3/CIS3 negatively regulate this migration. The results of this study suggest that LL-37 closes skin wounds by the induction of keratinocyte migration. *The Journal of Immunology,* **2005, 175: 4662–4668.**

Antimicrobial peptides are short amino acid sequences that can kill a variety of microbial pathogens. The major human antimicrobial peptides are the defensins and cathelicidin (1–4). Defensins are cysteine-rich cationic peptides and are further classified as α- or β-defensins based on structure. The α-defensins 1–4 (HNP1–4) are produced by neutrophils (5, 6), and the α-defensins 5 and 6 are found in Paneth cells of the gastrointestinal tract (7, 8). The β-defensins 1–4 (hBD 1–4)[4] are produced by epithelial tissues (9–12). hCAP18/LL-37 is the only human antimicrobial peptide that has been identified as a member of the cathelicidin family; it is produced in many tissues and cell types (4) and is processed to LL-37 in neutrophils (13). In the skin, epidermal keratinocytes produce hBD1–4 and hCAP18/LL-37 (4, 9–12). Murakami (14) analyzed sweat samples and identified three additional forms of cathelicidin peptide which deliver innate effector molecules in the absence of inflammation. Mast cells in the dermis were also found to produce hCAP18/LL-37 (15).

The epidermis plays an essential role in resistance against microbial-borne disease, as it is constantly exposed to a variety of microbial pathogens. The hBDs and hCAP18/LL-37 play major roles in this innate immune system (16). In addition, the epidermis functions as a physical barrier to microbial pathogens. However, once this physical barrier is disrupted by wounding, microbial pathogens can invade the underlying tissue. Therefore, the efficient closure of skin wounds is vital to the maintenance of homeostasis. In contrast, wounded skin expresses antimicrobial peptides, such as hCAP18/LL-37 and defensins (17–19). Although antimicrobial peptides were originally identified as molecules that kill microbial pathogens, there is strong evidence that these peptides have functions in antimicrobial immunity other than direct antimicrobial activity.

*Department of Dermatology, Ehime University School of Medicine, Ehime, Japan; †Department of Bacteriology, Hiroshima University Graduate School of Biomedical Sciences, Hiroshima, Japan; ‡Department of Molecular and Cellular Biology, Division of Biochemistry and Molecular Genetics, Ehime University School of Medicine, Ehime, Japan; and §Division of Molecular and Cellular Immunology, Medical Institute of Bioregulation, Kyushu University, Fukuoka, Japan

Received for publication March 10, 2005. Accepted for publication July 22, 2005.

The costs of publication of this article were defrayed in part by the payment of page charges. This article must therefore be hereby marked *advertisement* in accordance with 18 U.S.C. Section 1734 solely to indicate this fact.

[1] This work was supported by grants from the Ministries of Health, Labor, and Welfare and Education, Culture, Sports, Science, and Technology of Japan.

[2] S.T. and K.S. contributed equally to this article.

[3] Address correspondence and reprint requests to Dr. Koji Sayama, Department of Dermatology, Ehime University School of Medicine, Toon-City, Ehime 791-0295, Japan. E-mail address: sayama@m.ehime-u.ac.jp

[4] Abbreviations used in this paper: hBD, β-defensin; EGF, epidermal growth factor; EGFR, EGF receptor; HB-EGF, heparin-binding EGF; BHE, bovine hypothalamic extract; Ax, adenovirus vector; JAB, Jak2 binding; moi, multiplicity of infection; SOCS, suppressor of a cytokine signaling; CIS, cytokine-inducible Src homology 2-containing protein; STAT3F, dominant-negative mutants of STAT3; fPRL-1, formyl peptide receptor-like 1.

Copyright © 2005 by The American Association of Immunologists, Inc.

0022-1767/05/$02.00

Recently, it was revealed that these antimicrobial peptides are multifunctional proteins (20). Although hBDs are chemotactic for dendritic cells, LL-37 is chemotactic for neutrophils, monocytes, and T cells, but not for dendritic cells (3, 21, 22). LL-37 modulates dendritic cell differentiation and promotes Th1 responses (23). In the case of endothelial cells, LL-37 induces angiogenesis that is mediated by the formyl peptide receptor-like 1 receptor (24). In wounded skin, hCAP18/LL-37 is up-regulated, whereas the hCAP18/LL-37 levels in chronic ulcers are low (19). Furthermore, anti-LL-37 Ab inhibits re-epithelialization of skin wounds (19). These findings suggest that, apart from having antimicrobial activity, LL-37 plays an important role in wound healing.

The migration of epidermal keratinocytes is an important step in skin wound healing. Growth factors and the epidermal growth factor (EGF) receptor (EGFR) are involved in keratinocyte migration and proliferation (25, 26). Extracellular stimuli from the EGF and non-EGF families can activate the EGFR. These diverse stimuli include numerous agonists for heptahelical G-protein-coupled receptors, cytokines, and integrins (27, 28). The activation of the EGFR by non-EGFR ligands is called transactivation (27) and is mediated, at least in part, by heparin-binding EGF (HB-EGF), which is cleaved from its membrane-anchored form (pro-HB-EGF) by a specific metalloproteinase (29, 30). Recently, the transactivation of EGFR by LL-37 was reported for airway epithelial cells (31), which suggests that LL-37 induces keratinocyte migration via EGFR transactivation during skin wound healing.

The intracellular signaling molecule, STAT3, is involved in keratinocyte migration (32). The STAT family consists of STATs 1, 2, 3, 4, 5a, 5b, and 6. STATs and adaptor molecules are sequentially activated upon the binding of a cytokine to its receptor. After phosphorylation, STAT forms a homodimer or heterodimer, translocates into the nucleus, and initiates the transcription of target genes (33). These STAT signaling pathways are negatively regulated by the suppressor of a cytokine signaling (SOCS)/cytokine-inducible Src homology 2-containing protein (CIS) family, thereby avoiding oversignaling (34). In human keratinocytes, SOCS3/CIS3 negatively regulates hepatocyte growth factor-induced migration (35). Therefore, the STAT3-SOCS/CIS family may also be involved in LL-37-induced keratinocyte migration.

In this study, we demonstrate that LL-37 induces keratinocyte migration, and we examine the molecular mechanisms underlying EGFR transactivation.

Materials and Methods

Synthesis of LL-37

LL-37 was synthesized using a peptide synthesizer (Shimazu), as described previously (36). The peptide was purified using reverse-phase HPLC with an octadecyl-4PW column (Tosoh) and a linear gradient of aqueous 0.05% trifluoroacetic acid to 100% acetonitrile that contained 0.05% trifluoroacetic acid, and the sample was then lyophilized to remove the organic solvent. To confirm peptide purity and quality, mass spectrometry using the MALDI/TOF-mass spectrometry method was performed with Voyager (PerSeptive Biosystems). The peptides were assayed for LPS contamination by the *Limulus* test (Seikagaku).

Reagents and Abs

The following Abs were used: STAT3 (clone 84; BD Transduction Laboratories), phospho-STAT3 (no. 9131; Cell Signaling Technology), EGFR (clone 13; BD Transduction Laboratories), and phospho-EGFR (clone 9H2; Upstate Biotechnology) and EGFR neutralizing Ab (clone 225; Oncogene Research Products). AG1478 and CRM197 were purchased from Merck. OSU8-1 (37) was a gift from Canebo Science.

Keratinocyte culture

Primary normal human keratinocytes were isolated from normal human skin and cultured as previously described (38). The human skin samples were obtained after plastic surgery under a protocol approved by the Institutional Review Board of Ehime University School of Medicine. The skin samples were cut into 3- to 5-mm pieces and incubated with 250 U/ml dispase (Godoshusei) in DMEM overnight at 4°C. After separation of the epidermis from the dermis, the epidermal sheets were incubated in a 0.25% trypsin solution for 10 min at 37°C and teased with forceps. The keratinocytes were collected by centrifugation and were further cultured in MCDB153 medium that was supplemented with insulin (1 μg/ml), hydrocortisone (0.5 μM), ethanolamine (0.1 mM), phosphoethanolamine (0.1 mM), bovine hypothalamic extract (BHE; 50 μg/ml), and Ca^{2+} (0.1 mM). This supplement has been described elsewhere (39).

Migration assay

Keratinocyte migration was assayed quantitatively with a Boyden chamber, as described previously (40). Designated amounts of LL-37 were added to the bottom wells of a 48-well Boyden chamber (Neuro Probe), and an 8-μm pore-size polyvinylpyrrolidone-free polycarbonate membrane (Neuro Probe) was placed on the wells. The membrane was precoated with type I collagen (10 μg/ml in PBS; Nitta Gelatin) at room temperature for 1 h and then washed extensively with PBS. Subconfluent keratinocytes were harvested with trypsin-EDTA (0.05% trypsin and 0.5 mM EDTA) and resuspended in culture medium without BHE at 1×10^5 cells/ml. A 50-μl aliquot of the keratinocyte suspension (5,000 cells/well) was added to the upper wells, and the chamber was incubated overnight at 37°C in a humidified atmosphere of air with 5% CO_2. The cells that adhered to the upper surface of the filter membrane were removed by scraping with a rubber blade, and the cells that moved through the filter and stayed on the lower surface of the membrane were considered to be migrated cells. The membrane was fixed with 10% buffered formalin overnight and then stained overnight with Gill's hematoxylin. The membrane was then mounted between two glass slides with 90% glycerol, and the number of migrated cells was determined by counting under a microscope.

The role of EGFR transactivation in LL-37-induced keratinocyte migration was analyzed by the inhibition of EGFR transactivation with OSU8-1 (37), anti-EGFR neutralizing Ab no. 225, CRM197 (37), and AG1478. OSU8-1 (1 μM), anti-EGFR no. 225 (10 μg/ml), CRM197 (1 μg/ml), and AG1478 (30 nM) were added to the lower chamber together with 1 μg/ml LL-37, and LL-37-induced keratinocyte migration was analyzed as described previously.

Western blotting

Subconfluent keratinocytes were starved for 2 h in BHE-free medium and then stimulated with LL-37 as indicated. The cells were harvested on ice in lysis buffer that contained 5 mM EDTA, 100 μM sodium orthovanadate, 100 μM sodium pyrophosphate, 1 mM sodium fluoride, 5 μM 3,4-dichloroisocumarin, 1 μg/ml aprotinin, and 1% Triton X-100 in PBS. A 20-μg sample of protein was separated on 10% SDS-PAGE and then transferred to a polyvinylidene difluoride membrane. The membranes were blocked overnight at 4°C with 5% skimmed milk in PBS. The blocked membranes were incubated for 6 h with the first Ab as indicated. After three washes with PBS that contained 0.05% Tween 20, the membranes were treated with ABC reagents (Vector Laboratories) for 20 min at room temperature, washed three times with PBS that contained 0.05% Tween 20, treated with ECL detection reagents (Amersham Pharmacia Biotech) for 1 min at room temperature, and exposed to photographic film (Kodak).

Adenovirus vectors (Axs)

STAT3 has a phosphorylation site at tyrosine 705. In dominant-negative mutants of STAT3 (STAT3F), the phosphorylatable tyrosine residues are substituted with phenylalanine. Axs that encode STAT3F (AxCAStat3F), SOCS1/Jak2-binding (JAB) (AxCAJAB), and SOCS3/CIS3 (AxCACIS3) were generated as described previously (41), using the cosmid cassettes and Ad DNA-terminal protein complex method (42). An Ax that encodes lacZ (Ax LacZ) was a gift from Dr. I. Saito (University of Tokyo, Tokyo, Japan). Virus stocks were prepared using a standard procedure (42). Concentrated, purified virus stocks were prepared using a CsCl gradient, and the virus titer was checked using a plaque formation assay. We infected normal human keratinocytes with Axs at a multiplicity of infection (moi) of 5.

Statistical analyses

Data were collected from at least three independent experiments. Quantitative data are expressed as the mean ± SE. Statistical significance was determined by the paired Student t test. Differences were considered to be statistically significant for $p < 0.05$. The levels of statistical significance are indicated in the figures as follows: *, $p < 0.05$; **, $p < 0.01$.

Results

LL-37 induces keratinocyte migration

Initially, we investigated whether LL-37 induced keratinocyte migration. After the addition of 1 μg/ml LL-37 to cultured normal human keratinocytes, cell migration was observed by phase contrast microscopy. LL-37 induced keratinocyte migration at 12 h compared with the control (Fig. 1*A*). Next, we quantitatively analyzed LL-37-induced migration using the Boyden chamber assay (Fig. 1*B*). Various amounts of LL-37 and cultured keratinocytes were added to the lower and upper chambers, respectively. After incubation overnight, the migrated keratinocytes were counted. LL-37 induced a 3-fold increase in keratinocyte migration compared with the control treatment. The optimum concentration of LL-37 to induce migration was 1 μg/ml.

LL-37 phosphorylates EGFR

Because EGFR is involved in keratinocyte migration, we investigated whether EGFR transactivation is involved in LL-37-induced keratinocyte migration by analyzing the phosphorylation of EGFR by LL-37 (Fig. 2). LL-37 phosphorylated EGFR at 10 min, and the phosphorylation persisted for 15 min. The amount of EGFR protein did not change during this time period.

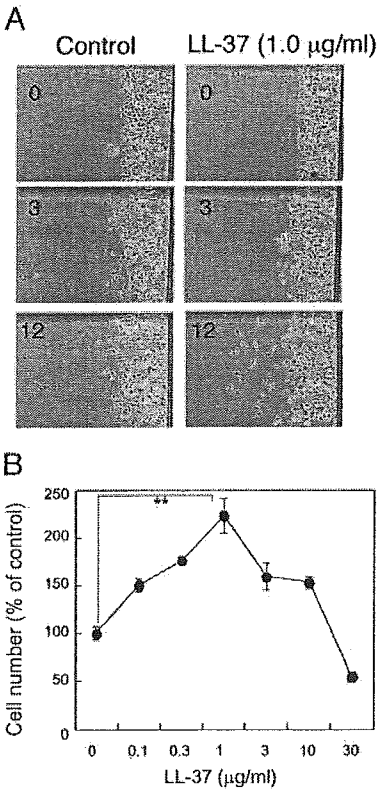

FIGURE 1. LL-37-induced keratinocyte migration. *A*, Keratinocyte migration was observed under the phase contrast microscope. A portion of the keratinocytes was removed from the tissue culture plates by scraping, and the remaining cells were cultured further with 1 μg/ml LL-37. The levels of cell migration were observed at 3 and 12 h. *B*, Keratinocyte migration was assayed quantitatively using the Boyden chamber. The indicated amounts of LL-37 were added to the bottom wells of a 48-well Boyden chamber, and an 8-μm pore-size polyvinylpyrrolidone-free polycarbonate membrane was placed on the wells. Keratinocytes were added to the upper wells at 5000 cells/well. After overnight incubation, the membrane was stained with Gill's hematoxylin. The number of cells that had migrated through the filter was determined by counting under a microscope. The data are shown as percentages of the control migration. Each point shows the mean ± SD of quadruplicate measurements. **, $p < 0.01$.

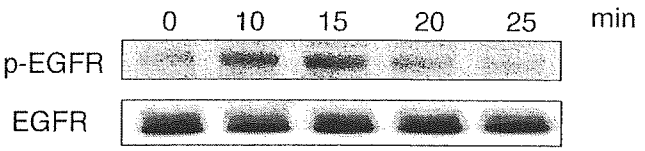

FIGURE 2. Activation of EGFR by LL-37. Phosphorylation of EGFR by LL-37. Subconfluent keratinocytes were starved for 2 h in BHE-free medium and stimulated with 1 μg/ml LL-37. The cells were harvested into lysis buffer at the indicated times. The phosphorylation of EGFR (p-EGFR) was analyzed by Western blotting. EGFR indicates total EGFR protein.

LL-37-induced keratinocyte migration occurs via HB-EGF-mediated EGFR transactivation

The activation of EGFR suggests that LL-37-induced keratinocyte migration is via EGFR transactivation. To confirm this suggestion, we used several inhibitors that block the sequential steps of EGFR transactivation (Figs. 3 and 4*B*). In EGFR transactivation, extracellular stimuli activate a metalloproteinase on the cell membrane, which cleaves the extracellular domain of the EGF family. The cleaved EGF then binds and phosphorylates EGFR, which transduces the signals into the intracellular signaling pathways. OSU8-1 is a metalloproteinase inhibitor that blocks the shedding of EGF family members (37). CRM197 is a nontoxic mutant of diphtheria toxin that binds to the extracellular domain of the membrane-anchored form of HB-EGF and inhibits the soluble form of HB-EGF, whereas it does not bind to other EGF family members, such as

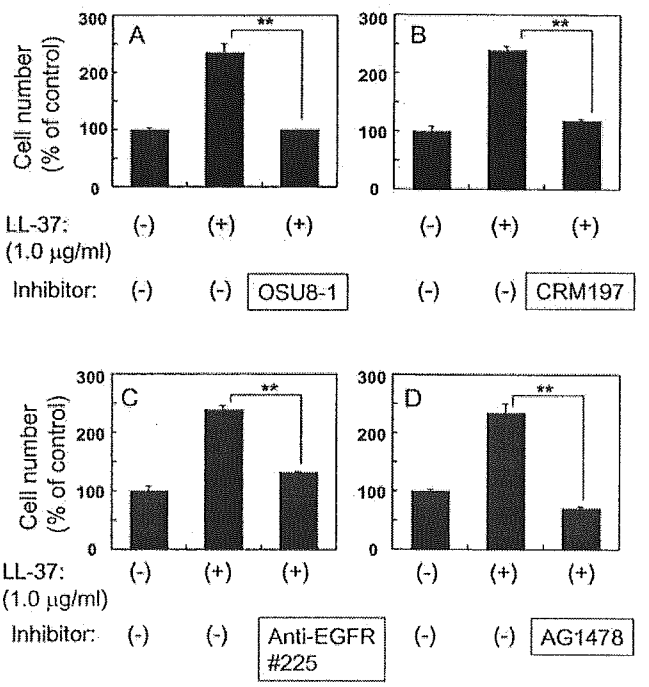

FIGURE 3. Inhibition of LL-37-induced keratinocyte migration by OSU8-1, CRM197, anti-EGFR no. 225, and AG1478. In the presence of inhibitors of EGFR transactivation, LL-37-induced keratinocyte migration was analyzed in the Boyden chamber assay. The mechanisms of action of these inhibitors are shown in Fig. 7. OSU8-1 (1 μM), CRM197 (1 μg/ml), anti-EGFR no. 225 (10 μg/ml), and AG1478 (30 nM) (*A–D*, respectively) were added to the lower chamber together with 1.0 μg/ml LL-37, and LL-37-induced keratinocyte migration was analyzed as described in Fig. 1. **, $p < 0.01$.

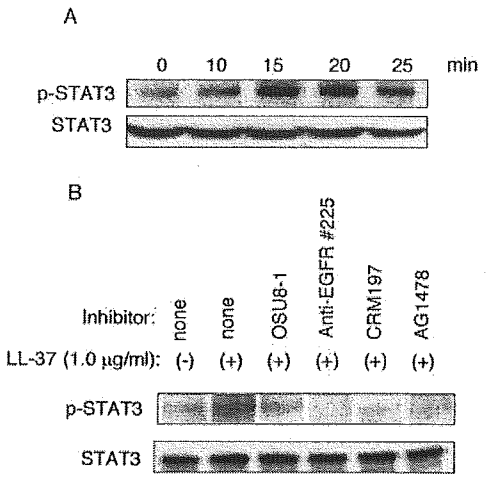

FIGURE 4. Phosphorylation of STAT3 by LL-37. *A*, Phosphorylation of STAT3 by LL-37. Subconfluent keratinocytes were starved for 2 h in BHE-free medium, and stimulated with 1 μg/ml LL-37. The cells were harvested into lysis buffer at the indicated time. The phosphorylation of STAT3 (p-STAT3) was analyzed by Western blotting. STAT3 indicates total STAT3 protein. *B*, Inhibition of LL-37-induced STAT3 phosphorylation by OSU8-1, anti-EGFR no. 225, CRM197, and AG1478. Keratinocytes were pretreated with OSU8-1 (1 μM), anti-EGFR no. 225 (10 μg/ml), CRM197 (1 μg/ml), or AG1478 (30 nM) for 1 h and then stimulated with 1 μg/ml LL-37 for 15 min. The phosphorylation of STAT3 was analyzed by Western blotting.

EGF, TGF-α, amphiregulin, and betacellulin (37). The anti-EGFR no. 225 Ab blocks the binding of EGF family members to the EGFR. AG1478 is an inhibitor of EGFR tyrosine kinase, which blocks the activation of EGFR.

Using these inhibitors, we investigated whether the inhibition of EGFR transactivation blocks LL-37-induced keratinocyte migration. After the addition of OSU8-1, CRM197, anti-EGFR no. 225, and AG1478 to the lower chamber with LL-37, keratinocyte migration was analyzed quantitatively using the Boyden chamber, as shown in Fig. 1. All of the inhibitors, including OSU8-1, CRM197, anti-EGFR no. 225, and AG1478, completely blocked LL-37-induced keratinocyte migration (Fig. 3). As LL-37 phosphorylates EGFR, and because LL-37-induced migration was completely blocked by OSU8-1, CRM197, anti-EGFR no. 225, and AG1478, we conclude that LL-37-induced keratinocyte migration is via HB-EGF-mediated EGFR transactivation.

LL-37 phosphorylates STAT3 via HB-EGF-mediated EGFR transactivation

A previous study has demonstrated that the STAT3 signaling pathway is involved in keratinocyte migration (32). Therefore, we studied the involvement of STAT3 in LL-37-induced keratinocyte migration. LL-37 maximally phosphorylated STAT3 at 15 min as determined by densitometric analysis, and the level of phosphorylation decreased at 25 min (Fig. 4). The amount of STAT3 protein did not change during this time. We also investigated whether LL-37-induced STAT3 phosphorylation occurred via HB-EGF-mediated EGFR transactivation. Keratinocytes were pretreated with OSU8-1, CRM197, anti-EGFR no. 225, and AG1478 for 1 h and were then stimulated with LL-37 for 15 min, followed by Western blot analysis. All of these inhibitors blocked LL-37-induced STAT3 phosphorylation, which again indicates that LL-37-induced STAT3 phosphorylation is via HB-EGF-mediated EGFR transactivation.

STAT3 is essential for LL-37-induced keratinocyte migration

We investigated whether STAT3 is essential for LL-37-induced keratinocyte migration. We constructed dominant-negative mutants of STAT3 (STAT3F) as well as Ax-carrying STAT3F (AxCAStat3F), as described previously (41). AxCAStat3F and the control vector AxLacZ were transfected (moi = 10) into keratinocytes. The expression of STAT3F almost completely blocked both LL-37-induced STAT3 phosphorylation and LL-37-induced keratinocyte migration (Fig. 5). Because STAT3 was phosphorylated by LL-37 and LL-37-induced migration was blocked by STAT3F, we conclude that the phosphorylation of STAT3 is essential for LL-37-induced keratinocyte migration.

SOCS1/JAB and SOCS3/CIS3 inhibit LL-37-induced keratinocyte migration

Because STAT3 is involved in LL-37-induced keratinocyte migration (as shown in Figs. 4 and 5), we analyzed the mechanism of regulation of STAT3 by SOCS1/JAB and SOCS3/CIS3. After the transfection of keratinocytes with AxCAJAB or AxCACIS3, LL-37-induced keratinocyte migration was analyzed quantitatively using the Boyden chamber assay (Fig. 6). The expression of either SOCS1/JAB or SOCS3/CIS3 almost completely blocked LL-37-induced keratinocyte migration. LL-37 induced neither SOCS1/JAB nor SOCS3/CIS3 (data not shown).

Discussion

The molecular mechanisms underlying LL-37-induced keratinocyte migration are summarized in Fig. 7. LL-37 activates the metalloproteinase, which cleaves the extracellular domain of HB-EGF. The soluble form of HB-EGF then binds to and phosphorylates EGFR. This, in turn, transduces the signals into the intracellular signaling pathways. STAT3 mediates this signaling pathway, leading to keratinocyte migration. SOCS1/JAB or SOCS3/CIS3 negatively regulates this STAT3 pathway and migration.

In a previous study, Tjabringa et al. (31) have shown that LL-37 activates airway epithelial cells, as demonstrated by its ability to activate ERK1/2 and to increase the release of IL-8. This activation

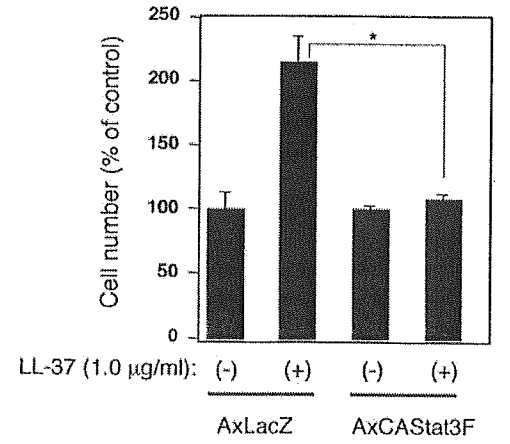

FIGURE 5. Inhibition of LL-37-induced keratinocyte migration by STAT3F. Ax LacZ and AxCAStat3F were transfected into normal human keratinocytes at a moi of 5. After 24 h, the keratinocytes were harvested and transferred to the upper well of the Boyden chamber. Then, 1 μg/ml LL-37 was added to the lower chamber, and keratinocyte migration was analyzed as described in Fig. 1. The numbers of migrated cells are shown as percentages of the control migration. Each point shows the mean ± SD of quadruplicate measurements. *, $p < 0.05$.

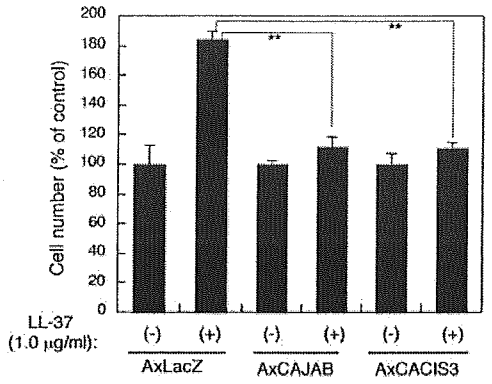

FIGURE 6. Inhibition of LL-37-induced keratinocyte migration by SOCS1/JAB and SOCS3/CIS3. Ax LacZ, AxCAJAB, and AxCACIS3 were transfected into normal human keratinocytes at a moi of 5. After 24 h, the keratinocytes were harvested and transferred to the upper well of the Boyden chamber. Then, 1 μg/ml LL-37 was added to the lower chamber, and keratinocyte migration was analyzed as described in Fig. 1. The numbers of migrated cells are shown as percentages of the control migration. Each point shows the mean ± SD of quadruplicate measurements. **, $p < 0.01$.

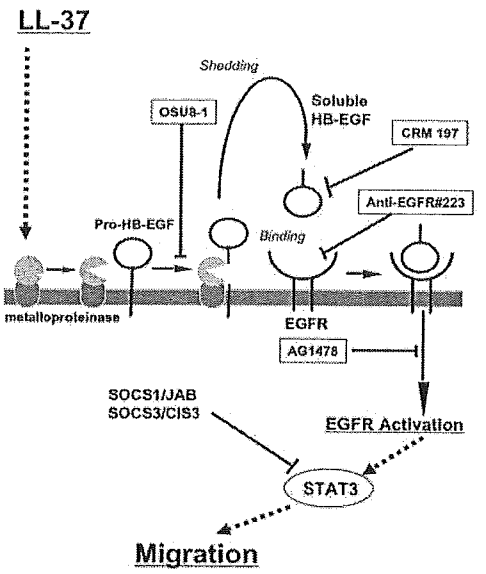

FIGURE 7. Proposed molecular mechanism of LL-37-induced keratinocyte migration. This scheme summarizes the pathway from LL-37 to keratinocyte migration and includes EGFR transactivation and STAT3. LL-37 activates the metalloproteinase, which cleaves the extracellular domain of HB-EGF. The soluble form of HB-EGF then binds and phosphorylates EGFR, which transduces the signals into the intracellular signaling pathways. OSU8-1 is a metalloproteinase inhibitor that blocks the shedding of EGF family proteins. CRM197 is a nontoxic mutant of diphtheria toxin that binds to the extracellular domain of the membrane-anchored form of HB-EGF; it inhibits the soluble form of HB-EGF but does not bind to the other EGF family members. The anti-EGFR no. 225 Ab blocks the binding of EGF family members to the EGFR. AG1478 is an inhibitor of EGFR tyrosine kinase, which blocks the activation of EGFR. OSU8-1, CRM197, anti-EGFR no. 225, and AG1478 all block LL-37-induced phosphorylation of EGFR and keratinocyte migration (Figs. 2 and 3), which indicates that the LL-37-induced EGFR activation occurs via HB-EGF-mediated EGFR transactivation. Following EGFR activation, keratinocyte migration is induced via STAT3 phosphorylation. SOCS1/JAB and SOCS3/CIS3 negatively regulate this STAT3 pathway.

requires the tyrosine kinase activity of the EGFR and involves the action of metalloproteinases and EGFR ligands, which indicates that the transactivation of EGFR is involved in this activation. The mechanism of this activation is quite similar to that of keratinocytes (Fig. 7). However, among the several EGFR ligands, no specific EGFR ligand for the transactivation of EGFR has been identified in airway epithelial cells. In keratinocytes, we found that HB-EGF is a mediator for LL-37-induced EGFR transactivation. The mechanism through which LL-37 activates metalloproteinase is still unclear. Several candidate molecules for the LL-37 receptor have been suggested, including the G protein-coupled formyl peptide receptor-like 1 (fPRL-1) (22, 24) and P2X7 (43). However, in airway epithelial cells, the activation was not inhibited by pertussis toxin or fPRL-1-antagonistic peptide, which indicates that fPRL-1 is not involved in transactivation of EGFR (31). Similarly, in keratinocytes, pertussis toxin did not inhibit LL-37-induced EGFR phosphorylation (data not shown), which suggests that fPRL-1 is not involved in LL-37-induced EGFR transactivation of keratinocytes. More recently, it has been suggested that LL-37 is able to cross the keratinocyte cell membrane and enter the cell (44). In this model, specific receptors are not required, and LL-37 may interact directly with the keratinocyte plasma membrane to cause conformational changes that activate indirectly a surface receptor that is linked to intracellular signaling molecules. If this is the case, it is possible that other highly cationic antimicrobial peptides, such as hBD1–3, also activate EGFR in keratinocytes. We tested this possibility and found that hBD1–3 phosphorylated EGFR in keratinocytes which suggests that the activation of keratinocytes is not unique to LL-37 among the antimicrobial peptides (our unpublished data).

The innate immune system is the first line of defense against microbial pathogens. Keratinocytes form a multilayered epidermis that separates the inner body from the outer environment and protects against a variety of microbial pathogens. Because the epidermis is the outermost layer of the body, epidermal keratinocytes are thought to be important components of innate immunity. Once the epidermis is disrupted by wounding, microbial pathogens can easily invade the body. Therefore, wound closure is an important issue for keratinocytes as participants in innate immunity. In this study, we have clearly demonstrated that LL-37 induces keratinocyte migration via EGFR transactivation. In the epidermis, bacterial contact, inflammation, and wounding are reported to stimulate keratinocytes to produce hCAP18/LL-37 (18, 36, 45). In addition to keratinocytes, granulocytes and skin mast cells produce hCAP18/LL-37 (4, 15). As hCAP18/LL-37 is up-regulated at the skin wound site (18), the present report strongly suggests that LL-37 induces keratinocyte migration to close the skin wound. In addition to its effects on keratinocytes, LL-37 can act on endothelial (24) and inflammatory cells, including neutrophils, monocytes, and T cells (22). Therefore, LL-37 may regulate skin wound healing through mechanisms that act directly on the cells within the wound environment rather than acting solely against microbial pathogens. Thus, hCAP18/LL-37 is a multifunctional mediator of innate immunity because it links host defenses and wound healing.

In the present study, the optimal concentration of LL-37 that induced keratinocyte migration was 1 μg/ml. The concentration of hCAP18/LL-37 at surgical wound sites has been reported to be ~2 μg/mg protein (19). Assuming that the protein concentration is similar to that in the serum (~70 mg/ml), the estimated concentration of hCAP18/LL-37 is 0.03 μg/ml. According to the data shown in Fig. 1, this concentration is insufficient to induce keratinocyte migration. However, immunohistochemical analysis has revealed that hCAP18/LL-37 is up-regulated, especially at the wound edge (19), which suggests that the local concentration of

LL-37 at the wound edge, where keratinocytes are migrating, may be high enough to induce migration.

Although we have shown that LL-37 induces keratinocyte migration, it has been reported that human serum inhibits the antimicrobial activity of LL-37 (46), which raises the possibility that serum also inhibits LL-37-induced keratinocyte migration during wound healing in vivo. In an ex vivo wound healing model, re-epithelialization occurred in two steps without inflammation, i.e., simple migration and subsequent proliferation of keratinocytes to form a provisional neoepidermis (19). Our data indicate that endogenous LL-37 mediates this keratinocyte migration. This ex vivo wound healing model requires medium that contains at least 10% FBS for re-epithelialization (47, 48). Furthermore, this re-epithelialization is inhibited by anti-LL-37 Ab (19), which indicates that endogenous LL-37 is a mediator of re-epithelialization even in the presence of serum. In addition to the ex vivo wound healing model, LL-37-induced migration of leukocytes is independent of the presence of serum (22). Therefore, LL-37-induced keratinocyte migration may not be hindered by the presence of serum or wound fluid in vivo.

Growth factors, such as insulin-like growth factor-I and TGF-α, have been shown to induce the expression of hCAP18/LL-37 and hBD3 in human keratinocytes (49). In addition to these growth factors, EGF family members, including HB-EGF, are known to induce hCAP18/LL-37 in keratinocytes (our unpublished data). The EGF family is thought to be involved in the re-epithelialization of skin wounds (50). Among the EGF family, HB-EGF is a major growth factor component of wound fluid (51). Wound stimuli induce the shedding of HB-EGF from keratinocytes (37). In contrast, the mechanism of induction of hCAP18/LL-37 is poorly understood (4). The induction of hCAP18/LL-37 by EGF family members suggests that the high level of expression of hCAP18/LL-37 on the keratinocytes at the wound edge is due to HB-EGF. In psoriasis, hCAP18/LL-37 is up-regulated in the lesional epidermis (52). Because EGF family expression is enhanced in the lesional skin of psoriasis patients (53, 54), these elevated levels of hCAP18/LL-37 may be due to increased levels of EGF family proteins.

We also analyzed the regulation of STAT3 activation during LL-37-induced keratinocyte migration. The SOCS/CIS family negatively regulates the STAT pathways (34, 55, 56). However, the inhibitory functions of the SOCS/CIS family differ according to the cell type and cellular conditions. In this study, we showed that SOCS1/JAB or SOCS3/CIS3 block LL-37-induced keratinocyte migration, which suggests that migration is inhibited under conditions of high-level SOCS1/JAB or SOCS3/CIS3. Cytokines, such as IFN-γ, IL-4, and IL-6, have been implicated in a variety of physiological and pathological conditions of the skin. IFN-γ enhances SOCS1/JAB and SOCS3/CIS3 expression (41) in normal human keratinocytes. In addition, IL-4 and IL-6 enhance the expression of SOCS1/JAB and SOCS3/CIS3, respectively, in normal human keratinocytes (41). Therefore, the possibility exists that IFN-γ, IL-4, and IL-6 affect wound healing in various inflammatory skin conditions by regulating keratinocyte migration via the induction of SOCS1/JAB or SOCS3/CIS3, which would lead to sustained wound healing in chronic ulcers. However, SOCS1/JAB and SOCS3/CIS3 were not induced by LL-37, which indicates that SOCS1/JAB and SOCS3/CIS3 do not act as self-limiting factors in LL-37-induced keratinocyte migration.

In conclusion, LL-37 induces keratinocyte migration via HB-EGF-mediated EGFR transactivation and STAT3 phosphorylation.

Acknowledgments

We thank Teruko Tsuda and Eriko Tan for significant technical assistance.

Disclosures

The authors have no financial conflict of interest.

References

1. Ganz, T. 2003. Defensins: antimicrobial peptides of innate immunity. *Nat. Rev. Immunol.* 3: 710–720.
2. Lehrer, R. I., and T. Ganz. 1999. Antimicrobial peptides in mammalian and insect host defence. *Curr. Opin. Immunol.* 11: 23–27.
3. Yang, D., O. Chertov, and J. J. Oppenheim. 2001. Participation of mammalian defensins and cathelicidins in anti-microbial immunity: receptors and activities of human defensins and cathelicidin (LL-37). *J. Leukocyte Biol.* 69: 691–697.
4. Zaiou, M., and R. L. Gallo. 2002. Cathelicidins, essential gene-encoded mammalian antibiotics. *J. Mol. Med.* 80: 549–561.
5. Ganz, T., M. E. Selsted, D. Szklarek, S. S. Harwig, K. Daher, D. F. Bainton, and R. I. Lehrer. 1985. Defensins: natural peptide antibiotics of human neutrophils. *J. Clin. Invest.* 76: 1427–1435.
6. Selsted, M. E., S. S. Harwig, T. Ganz, J. W. Schilling, and R. I. Lehrer. 1985. Primary structures of three human neutrophil defensins. *J. Clin. Invest.* 76: 1436–1439.
7. Jones, D. E., and C. L. Bevins. 1993. Defensin-6 mRNA in human paneth cells: implications for antimicrobial peptides in host defense of the human bowel. *FEBS Lett.* 315: 187–192.
8. Quayle, A. J., E. M. Porter, A. A. Nussbaum, Y. M. Wang, C. Brabec, K. P. Yip, and S. C. Mok. 1998. Gene expression, immunolocalization, and secretion of human defensin-5 in human female reproductive tract. *Am. J. Pathol.* 152: 1247–1258.
9. Harder, J., J. Bartels, E. Christophers, and J. M. Schroder. 2001. Isolation and characterization of human β-defensin-3, a novel human inducible peptide antibiotic. *J. Biol. Chem.* 276: 5707–5713.
10. Harder, J., J. Bartels, E. Christophers, and J.-M. Schroder. 1997. A peptide antibiotic from human skin. *Nature* 387: 861.
11. Valore, E. V., C. H. Park, A. J. Quayle, K. R. Wiles, P. B. McCray, Jr., and T. Ganz. 1998. Human β-defensin-1: an antimicrobial peptide of urogenital tissues. *J. Clin. Invest.* 101: 1633–1642.
12. Harder, J., U. Meyer-Hoffert, K. Wehkamp, L. Schwichtenberg, and J. M. Schroder. 2004. Differential gene induction of human β-defensins (hBD-1, -2, -3, and -4) in keratinocytes is inhibited by retinoic acid. *J. Invest. Dermatol.* 123: 522–529.
13. Sorensen, O. E., P. Follin, A. H. Johnsen, J. Calafat, G. S. Tjabringa, P. S. Hiemstra, and N. Borregaard. 2001. Human cathelicidin, hCAP-18, is processed to the antimicrobial peptide LL-37 by extracellular cleavage with proteinase 3. *Blood* 97: 3951–3959.
14. Murakami, M., T. Ohtake, R. A. Dorschner, B. Schittek, C. Garbe, and R. L. Gallo. 2002. Cathelicidin anti-microbial peptide expression in sweat, an innate defense system for the skin. *J. Invest. Dermatol.* 119: 1090–1095.
15. Di Nardo, A., A. Vitiello, and R. L. Gallo. 2003. Cutting edge: mast cell antimicrobial activity is mediated by expression of cathelicidin antimicrobial peptide. *J. Immunol.* 170: 2274–2278.
16. Nizet, V., T. Ohtake, X. Lauth, J. Trowbridge, J. Rudisill, R. A. Dorschner, V. Pestonjamasp, J. Piraino, K. Huttner, and R. L. Gallo. 2001. Innate antimicrobial peptide protects the skin from invasive bacterial infection. *Nature* 414: 454–457.
17. Frohm, M., H. Gunne, A. C. Bergman, B. Agerberth, T. Bergman, A. Boman, S. Liden, H. Jornvall, and H. G. Boman. 1996. Biochemical and antibacterial analysis of human wound and blister fluid. *Eur. J. Biochem.* 237: 86–92.
18. Dorschner, R. A., V. K. Pestonjamasp, S. Tamakuwala, T. Ohtake, J. Rudisill, V. Nizet, B. Agerberth, G. H. Gudmundsson, and R. L. Gallo. 2001. Cutaneous injury induces the release of cathelicidin anti-microbial peptides active against group A *Streptococcus*. *J. Invest. Dermatol.* 117: 91–97.
19. Heilborn, J. D., M. F. Nilsson, G. Kratz, G. Weber, O. Sorensen, N. Borregaard, and M. Stahle-Backdahl. 2003. The cathelicidin anti-microbial peptide LL-37 is involved in re-epithelialization of human skin wounds and is lacking in chronic ulcer epithelium. *J. Invest. Dermatol.* 120: 379–389.
20. Elsbach, P. 2003. What is the real role of antimicrobial polypeptides that can mediate several other inflammatory responses? *J. Clin. Invest.* 111: 1643–1645.
21. Yang, D., O. Chertov, S. N. Bykovskaia, Q. Chen, M. J. Buffo, J. Shogan, M. Anderson, J. M. Schroder, J. M. Wang, O. M. Howard, and J. J. Oppenheim. 1999. β-Defensins: linking innate and adaptive immunity through dendritic and T cell CCR6. *Science* 286: 525–528.
22. De, Y., Q. Chen, A. P. Schmidt, G. M. Anderson, J. M. Wang, J. Wooters, J. J. Oppenheim, and O. Chertov. 2000. LL-37, the neutrophil granule- and epithelial cell-derived cathelicidin, utilizes formyl peptide receptor-like 1 (FPRL1) as a receptor to chemoattract human peripheral blood neutrophils, monocytes, and T cells. *J. Exp. Med.* 192: 1069–1074.
23. Davidson, D. J., A. J. Currie, G. S. Reid, D. M. Bowdish, K. L. MacDonald, R. C. Ma, R. E. Hancock, and D. P. Speert. 2004. The cationic antimicrobial peptide LL-37 modulates dendritic cell differentiation and dendritic cell-induced T cell polarization. *J. Immunol.* 172: 1146–1156.
24. Koczulla, R., G. von Degenfeld, C. Kupatt, F. Krotz, S. Zahler, T. Gloe, K. Issbrucker, P. Unterberger, M. Zaiou, C. Lebherz, et al. 2003. An angiogenic role for the human peptide antibiotic LL-37/hCAP-18. *J. Clin. Invest.* 111: 1665–1672.
25. Sarret, Y., D. T. Woodley, K. Grigsby, K. Wynn, and E. J. O'Keefe. 1992. Human keratinocyte locomotion: the effect of selected cytokines. *J. Invest. Dermatol.* 98: 12–16.

26. McCawley, L. J., P. O'Brien, and L. G. Hudson. 1997. Overexpression of the epidermal growth factor receptor contributes to enhanced ligand-mediated motility in keratinocyte cell lines. *Endocrinology* 138: 121–127.
27. Daub, H., F. U. Weiss, C. Wallasch, and A. Ullrich. 1996. Role of transactivation of the EGF receptor in signalling by G-protein-coupled receptors. *Nature* 379: 557–560.
28. Miyamoto, S., H. Teramoto, J. S. Gutkind, and K. M. Yamada. 1996. Integrins can collaborate with growth factors for phosphorylation of receptor tyrosine kinases and MAP kinase activation: roles of integrin aggregation and occupancy of receptors. *J. Cell Biol.* 135: 1633–1642.
29. Prenzel, N., E. Zwick, H. Daub, M. Leserer, R. Abraham, C. Wallasch, and A. Ullrich. 1999. EGF receptor transactivation by G-protein-coupled receptors requires metalloproteinase cleavage of proHB-EGF. *Nature* 402: 884–888.
30. Asakura, M., M. Kitakaze, S. Takashima, Y. Liao, F. Ishikura, T. Yoshinaka, H. Ohmoto, K. Node, K. Yoshino, H. Ishiguro, et al. 2002. Cardiac hypertrophy is inhibited by antagonism of ADAM12 processing of HB-EGF: metalloproteinase inhibitors as a new therapy. *Nat. Med.* 8: 35–40.
31. Tjabringa, G. S., J. Aarbiou, D. K. Ninaber, J. W. Drijfhout, O. E. Sorensen, N. Borregaard, K. F. Rabe, and P. S. Hiemstra. 2003. The antimicrobial peptide LL-37 activates innate immunity at the airway epithelial surface by transactivation of the epidermal growth factor receptor. *J. Immunol.* 171: 6690–6696.
32. Sano, S., S. Itami, K. Takeda, M. Tarutani, Y. Yamaguchi, H. Miura, K. Yoshikawa, S. Akira, and J. Takeda. 1999. Keratinocyte-specific ablation of Stat3 exhibits impaired skin remodeling, but does not affect skin morphogenesis. *EMBO J.* 18: 4657–4668.
33. Leonard, W. J., and J. J. O'Shea. 1998. Jaks and STATs: biological implications. *Annu. Rev. Immunol.* 16: 293–322.
34. Duhe, R. J., L. H. Wang, and W. L. Farrar. 2001. Negative regulation of Janus kinases. *Cell Biochem. Biophys.* 34: 17–59.
35. Tokumaru, S., K. Sayama, K. Yamasaki, Y. Shirakata, Y. Hanakawa, Y. Yahata, X. Dai, M. Tohyama, L. Yang, A. Yoshimura, and K. Hashimoto. 2005. SOCS3/CIS3 negative regulation of STAT3 in HGF-induced keratinocyte migration. *Biochem. Biophys. Res. Commun.* 327: 100–105.
36. Midorikawa, K., K. Ouhara, H. Komatsuzawa, T. Kawai, S. Yamada, T. Fujiwara, K. Yamazaki, K. Sayama, M. A. Taubman, H. Kurihara, et al. 2003. *Staphylococcus aureus* susceptibility to innate antimicrobial peptides, β-defensins and CAP18, expressed by human keratinocytes. *Infect. Immun.* 71: 3730–3739.
37. Tokumaru, S., S. Higashiyama, T. Endo, T. Nakagawa, J. I. Miyagawa, K. Yamamori, Y. Hanakawa, H. Ohmoto, K. Yoshino, Y. Shirakata, et al. 2000. Ectodomain shedding of epidermal growth factor receptor ligands is required for keratinocyte migration in cutaneous wound healing. *J. Cell Biol.* 151: 209–220.
38. Sayama, K., Y. Shirakata, K. Midorikawa, Y. Hanakawa, and K. Hashimoto. 1999. Possible involvement of p21 but not of p16 or p53 in keratinocyte senescence. *J. Cell Physiol.* 179: 40–44.
39. Shirakata, Y., H. Ueno, Y. Hanakawa, K. Kameda, K. Yamasaki, S. Tokumaru, Y. Yahata, M. Tohyama, K. Sayama, and K. Hashimoto. 2004. TGF-β is not involved in early phase growth inhibition of keratinocytes by 1α,25(OH)2vitamin D3. *J. Dermatol. Sci.* 36: 41–50.
40. Boyden, S. 1962. The chemotactic effect of mixtures of antibody and antigen on polymorphonuclear leucocytes. *J. Exp. Med.* 115: 453–466.
41. Yamasaki, K., Y. Hanakawa, S. Tokumaru, Y. Shirakata, K. Sayama, T. Hanada, A. Yoshimura, and K. Hashimoto. 2003. Suppressor of cytokine signaling 1/JAB and suppressor of cytokine signaling 3/cytokine-inducible SH2 containing protein 3 negatively regulate the signal transducers and activators of transcription signaling pathway in normal human epidermal keratinocytes. *J. Invest. Dermatol.* 120: 571–580.
42. Miyake, S., M. Makimura, Y. Kanegae, S. Harada, Y. Sato, K. Takamori, C. Tokuda, and I. Saito. 1996. Efficient generation of recombinant adenoviruses using adenovirus DNA-terminal protein complex and a cosmid bearing the full-length virus genome. *Proc. Natl. Acad. Sci. USA* 93: 1320–1324.
43. Elssner, A., M. Duncan, M. Gavrilin, and M. D. Wewers. 2004. A novel P2X7 receptor activator, the human cathelicidin-derived peptide LL37, induces IL-1β processing and release. *J. Immunol.* 172: 4987–4994.
44. Braff, M. H., M. A. Hawkins, A. Di Nardo, B. Lopez-Garcia, M. D. Howell, C. Wong, K. Lin, J. E. Streib, R. Dorschner, D. Y. Leung, and R. L. Gallo. 2005. Structure-function relationships among human cathelicidin peptides: dissociation of antimicrobial properties from host immunostimulatory activities. *J. Immunol.* 174: 4271–4278.
45. Frohm, M., B. Agerberth, G. Ahangari, M. Stahle-Backdahl, S. Liden, H. Wigzell, and G. H. Gudmundsson. 1997. The expression of the gene coding for the antibacterial peptide LL-37 is induced in human keratinocytes during inflammatory disorders. *J. Biol. Chem.* 272: 15258–15263.
46. Johansson, J., G. H. Gudmundsson, M. E. Rottenberg, K. D. Berndt, and B. Agerberth. 1998. Conformation-dependent antibacterial activity of the naturally occurring human peptide LL-37. *J. Biol. Chem.* 273: 3718–3724.
47. Inoue, M., G. Kratz, A. Haegerstrand, and M. Stahle-Backdahl. 1995. Collagenase expression is rapidly induced in wound-edge keratinocytes after acute injury in human skin, persists during healing, and stops at re-epithelialization. *J. Invest. Dermatol.* 104: 479–483.
48. Kratz, G. 1998. Modeling of wound healing processes in human skin using tissue culture. *Microsc. Res. Tech.* 42: 345–350.
49. Sorensen, O. E., J. B. Cowland, K. Theilgaard-Monch, L. Liu, T. Ganz, and N. Borregaard. 2003. Wound healing and expression of antimicrobial peptides/polypeptides in human keratinocytes, a consequence of common growth factors. *J. Immunol.* 170: 5583–5589.
50. Martin, P. 1997. Wound healing–aiming for perfect skin regeneration. *Science* 276: 75–81.
51. Marikovsky, M., K. Breuing, P. Y. Liu, E. Eriksson, S. Higashiyama, P. Farber, J. Abraham, and M. Klagsbrun. 1993. Appearance of heparin-binding EGF-like growth factor in wound fluid as a response to injury. *Proc. Natl. Acad. Sci. USA* 90: 3889–3893.
52. Ong, P. Y., T. Ohtake, C. Brandt, I. Strickland, M. Boguniewicz, T. Ganz, R. L. Gallo, and D. Y. Leung. 2002. Endogenous antimicrobial peptides and skin infections in atopic dermatitis. *N. Engl. J. Med.* 347: 1151–1160.
53. Elder, J. T., G. J. Fisher, P. B. Lindquist, G. L. Bennett, M. R. Pittelkow, R. J. Coffey, Jr., L. Ellingsworth, R. Derynck, and J. J. Voorhees. 1989. Overexpression of transforming growth factor α in psoriatic epidermis. *Science* 243: 811–814.
54. Cook, P. W., M. R. Pittelkow, W. W. Keeble, R. Graves-Deal, R. J. Coffey, Jr., and G. D. Shipley. 1992. Amphiregulin messenger RNA is elevated in psoriatic epidermis and gastrointestinal carcinomas. *Cancer Res.* 52: 3224–3227.
55. Naka, T., M. Narazaki, M. Hirata, T. Matsumoto, S. Minamoto, A. Aono, N. Nishimoto, T. Kajita, T. Taga, K. Yoshizaki, et al. 1997. Structure and function of a new STAT-induced STAT inhibitor. *Nature* 387: 924–929.
56. Alexander, W. S., R. Starr, J. E. Fenner, C. L. Scott, E. Handman, N. S. Sprigg, J. E. Corbin, A. L. Cornish, R. Darwiche, C. M. Owczarek, et al. 1999. SOCS1 is a critical inhibitor of interferon γ signaling and prevents the potentially fatal neonatal actions of this cytokine. *Cell* 98: 597–608.

Urokinase-induced activation of the gp130/Tyk2/Stat3 pathway mediates a pro-inflammatory effect in human mesangial cells via expression of the anaphylatoxin C5a receptor

Nelli Shushakova[1], Natalia Tkachuk[1], Marc Dangers[1], Sergey Tkachuk[1], Joon-Keun Park[1], Joerg Zwirner[2], Koji Hashimoto[3], Hermann Haller[1] and Inna Dumler[1,4,*]

[1]Hannover Medical School, Carl-Neuberg Straße 1, 30625 Hannover, Germany
[2]Department of Immunology, Georg-August-University, Kreuzbergring 57, 37073 Göttingen, Germany
[3]Ehime University School of Medicine, Shitsukawa, Shigenobucho, Onsengun, Ehime 791-0295, Japan
[4]Medical Faculty of the Charité–Franz Volhard Clinic, HELIOS Klinikum-Berlin and Max Delbrück Center for Molecular Medicine, Wiltbergstrasse 50, 13125 Berlin, Germany
*Author for correspondence (e-mail: dumler.inna@mh-hannover.de)

Accepted 30 March 2005
Journal of Cell Science 118, 2743-2753 Published by The Company of Biologists 2005
doi:10.1242/jcs.02409

Summary

Glomerular mesangial cells (MCs) are central to the pathogenesis of progressive glomeruli-associated renal diseases. However, molecular mechanisms underlying changes in MC functions still remain poorly understood. Here, we show that in MCs, the urokinase-type plasminogen activator (uPA) induces, via its specific receptor (uPAR, CD87), upregulated expression of the complement anaphylatoxin C5a receptor (C5aR, CD88), and modulates C5a-dependent functional responses. This effect is mediated via the interaction of the uPA-specific receptor (uPAR, CD87) and gp130, a signal transducing subunit of the receptor complexes for the IL-6 cytokine family. The Janus kinase Tyk2 and the transcription factor Stat3 serve as downstream components in the signaling cascade resulting in upregulation of C5aR expression. In vivo, expression of C5aR and uPAR was increased in the mesangium of wild-type mice in a lipopolysaccharide (LPS)-induced model of inflammation, whereas in *uPAR*$^{-/-}$ animals C5aR expression remained unchanged. This is the first demonstration in vitro and in vivo that uPA acts in MCs as a modulator of immune responses via control of immune-competent receptors. The data suggest a novel role for uPA/uPAR in glomeruli-associated renal failure via a signaling cross-talk between the fibrinolytic and immune systems.

Key words: Urokinase, uPA receptor, C5a receptor, Mesangial cells, Inflammation

Introduction

The early stages of inflammatory processes are accompanied by activation of the complement system. One of the biological consequences of this activation is the release of potent inflammatory molecules, C3a and C5a anaphylatoxins. Anaphylatoxins act through specific receptors that are members of the rhodopsin family of seven transmembrane-spanning G protein-linked receptors (Gerard and Gerard, 1994). Expression of these receptors, initially thought to be restricted to peripheral blood leukocytes, appears to occur in several tissues. Recent reports provide evidence for the expression of anaphylatoxin C5a receptor (C5aR, CD88) on human mesangial cells (MCs), which play a pivotal role in renal physiology (Braun and Davis III, 1998; Wilmer et al., 1998). Moreover, C5aR activation in MCs induced proliferation, selective production of cytokines and growth factors, as well as upregulation of certain transcription factors and early response genes (Wilmer et al., 1998). All these parameters might determine the degree of mesangial injury, which in turn dictates the final outcome of the inflammatory process. These data indicate a role for the MC-expressed C5aR in mediating glomerular injury and pathogenesis of progressive glomeruli-associated renal diseases. This implication is strengthened by the demonstration of enhanced expression of C5aR in human diseased kidney (Abe et al., 2001) and by the recent studies on C5aR-mediated renal dysfunction (de Vries et al., 2003; Aramugam et al., 2003). However, molecular mechanisms of MC stimulation and upregulated C5aR expression in MCs remain unexplored. Most probably important candidates might be complement proteins, platelet products and components of the fibrinolytic system, in particular the urokinase-type plasminogen activator (uPA) and its specific receptor (uPAR, CD87).

uPA is a multifunctional molecule that serves either as a proteolytic enzyme or as a signal-inducing ligand. The urokinase receptor uPAR was originally identified as a proteinase receptor for uPA, directing pericellular proteolysis. However, uPAR also mediates intracellular signaling via surface proteins such as integrins, growth factors receptors and G-protein-coupled membrane proteins. These dual properties enable the uPA/uPAR system to control pericellular fibrinolytic and proteolytic activities, as well as cell adhesion, migration, proliferation and differentiation (Blasi and Carmeliet, 2002).

Journal of Cell Science

Journal of Cell Science

Moreover, recent findings in vitro and in vivo indicate that the uPA/uPAR system is an active participant in the majority of infection and inflammatory diseases and might serve as a modulator of immunological responses (Gyetko et al., 1996; Gyetko et al., 2000; May et al., 1998; Mondino and Blasi, 2004). Remarkably, modulating effects of the uPA/uPAR system on immunological responses may involve not only migration of different types of leukocytes to the site of inflammation but also contribute to generating pro- and anti-inflammatory signals, such as TNF-α neo-synthesis of lipopolysaccharide (LPS)-stimulated mononuclear phagocytes in vitro (Sitrin et al., 1996) and IFN-γ and IL-12 in vivo in response to pulmonary infection (Gyetko et al., 2002). Moreover, in the murine model of endotoxemia-induced lung injury, uPA increases LPS-induced activation of neutrophils via activation of a uPAR-directed intracellular signaling pathways including Akt and c-Jun N-terminal kinase, nuclear translocation of NF-κB and enhanced expression of IL-1β, TNF-α and MIP-2 (Abraham et al., 2003). These data suggest the interplay of the uPA/uPAR system and transcription factors that may represent an important cell-specific mechanism that upregulates the inflammatory response and facilitates MC proliferation upon progressive glomerular diseases.

In this study we show that through Tyk2/Stat3 activation, uPAR occupancy by uPA and its association with gp130 protein, a signal transducing subunit of the IL-6 receptor complexes, upregulates expression of anaphylatoxin C5aR on human MCs and modulates C5aR-dependent functional cell responses. These findings identify components of a novel pathway that couples fibrinolytic and immune systems in kidney inflammatory diseases.

Materials and Methods

Materials

Chemicals of high quality commercial grade were purchased from Sigma, Amersham Bioscience Inc., Merck, Serva (Heidelberg, Germany), Carl Roth GmbH (Karlsruhe, Germany) and Bio-Rad Laboratories (Hercules, CA, USA). Chemiluminescent signal enhancer was obtained from Perkin Elmer Life Sciences (Boston, MA, USA). Mounting medium was purchased from Polysciences, Inc. (Warrington, PA, USA). uPA was from Loxo (Dossenheim, Germany).

Antibodies

Anti-human CD88, anti-human gp130 and horseradish peroxidase-conjugated secondary polyclonal antibodies were from Santa Cruz Biotechnology, Inc. (Santa Cruz, CA, USA). Anti-STAT3 and anti-Tyk2 monoclonal antibodies were from Transduction Laboratories (Lexington, KY, USA), anti-phospho-STAT3 (Tyr705) and anti-phospho-Tyk2 (Tyr1054/1055) polyclonal antibodies were from Cell Signaling Technology (Beverly, MA, USA). Monoclonal anti-human uPAR clone R3 antibody was from Monozyme (Copenhagen, Denmark). Alexa Fluor 488-conjugated goat anti-rabbit and Alexa Fluor 488-conjugated donkey anti-goat antibodies were purchased from Molecular Probes, Inc. (Eugene, OR, USA). Normal rabbit IgG and normal mouse IgG were from Upstate Biotechnology, Inc. (Lake Plasid, NY, USA). Monoclonal anti-mouse C5aR antibodies (clone 2/70, rat anti-mouse IgG) were generated as described previously (Werfel et al., 1996).

Cell culture

Normal human mesangial cells were obtained from Clonetics (San Diego, CA, USA). The cells were cultured in MsGM medium (Clonetics) supplemented with 5% fetal bovine serum (Clonetics) and were used in passage 8. For the uPA stimulation experiments, cells were starved for 24 hours in serum-free medium. For inhibition experiments cells were pretreated before uPA stimulation for 1 hour with the appropriate antibody at 5 μg/ml medium.

Cell infection, Tyk2 and Stat3 expression

Adenoviral Tyk2 constructs were generated as previously described (Kusch et al., 2000). Additionally, the deletion mutant Ad5Tyk2ΔC was generated by removing the kinase domain after amino acid 776. As a control, an adenovirus expressing β-galactosidase (Ad5βGal) was used. Adenoviral Stat3F construct with a point mutation in the tyrosine phosphorylation site at residue 705 (Tyr to Phe) was generated as previously described (Yahata et al., 2003). Cells were grown up to 80% confluency and infected for 1 hour with recombinant adenovirus stock at a multiplicity of infection of 500 plaque-forming units/cell in a total volume of 1 ml/well in six-well plates. The efficiency of infection was assessed by western blotting using anti-Tyk2 or anti-Stat3 antibody, respectively. Cells were serum-starved overnight after 24 hours of infection and used for experiments on the second day after infection. Total RNA was prepared using an RNeasy Kit (QIAGEN GmbH, Germany).

Design and cloning of lentiviral siRNA vectors

The human *uPAR* cDNA sequence (NM 002659) was searched for suitable siRNA target sequences starting with aag followed by 18 nucleotides. The 21 nucleotides sense and antisense sequences were subjected to BLAST searches, eliminating sequences with more than 16 bp homologies in the human genome. uPAR siRNA oligonucleotides (uPARsi): sense, 5′-GATCCCC**AAGCTGTACCCACTCAGAG**TTCAAGAGA**CTCTGAGTGGGTACAGCTT**TTTTTGGAAA; antisense, 5′-AGCTTTTCCAAAAA**AAGCTGTACCCACTCAGAG**TCTCTTGAA**CTCTGAGTGGGTACAGCTT**GGG. Sense and antisense siRNA sequences are shown in bold and loop sequences are underlined. Hybridized oligonucleotides were ligated into the pSuper.retro vector (purchased from Oligo Engine, Seattle, WA, USA), into the *Bgl*II-*Hin*dIII-site, downstream of the H1 promoter. The H1-hairpin-precursor cassette was excised from pSuper.retro with *Eco*RI and *Cla*I (Fermentas GmbH, Germany) and further cloned into *Eco*RI-*Cla*I site of the pLV-TH plasmid.

Lentiviral vector production and cell infection

Lentiviral vectors were produced by transient transfection of 293T cells according to standard protocols. Briefly, 293T cells were cultured in Dulbecco's modified Eagle's medium (DMEM), supplemented with 10% fetal calf serum (FCS) and, when subconfluent, transfected with 15 μg of pCMV-ΔR8.91, 6 μg of pMD2G and 20 μg of pLV-TH-uPARsi, or pLV-TH as control. The transfection was performed by calcium-phosphate precipitation. Medium was changed to DMEM, supplemented with 2% FCS, after 6 to 8 hours. Vector supernatants, containing viral particles, were harvested approximately 48 hours later and concentrated by ultracentrifugation (1.5 hours at 25,000 *g* at 4°C). The virus obtained was assigned as LV-uPARsi. The viral batches were titered on 293 cells. MCs were infected in the presence of 8 μg/ml polybrene with viruses at 10^8 TU/ml and used for experiments day 3 after infection. 95% of cells have been shown to be infected under these conditions.

Quantitative RT-PCR analysis of C5aR in human MCs

The total RNA was isolated from human MCs and real-time quantitative RT-PCR for C5aR was performed on a TaqMan ABI 7700 Sequence Detection System (Applied Biosystems, Foster City, CA,

Journal of Cell Science

USA). *GAPDH* was used as a reference gene. The following oligonucleotide primers and probes were used: GAPDH, 5′-GAAGGTGAAGGTCGGAGTC-3′ (sense), 5′-GAAGATGGTGATGGGATTC-3′ (antisense), 6-FAM-CAAGCTTCCCGTTCTCAGCC-TAMRA (probe); C5aR, 5′-GTGGTCCGGGAGGAGTACTTT-3′ (sense), 5′-GCCGTTTGTCGTGGCTGTA-3′ (antisense), 6-FAM-CACCAAAGGTGTTGTGTGGCGTGG-TAMRA (probe).

Immunoprecipitation and western blotting

Subconfluent, serum-starved MCs were treated with 10 nM uPA for 5-30 minutes at 37°C, lysed in RIPA buffer containing 1 mM Na_3VO_4, 1 mM NaF, 1 mM PMSF, 10 μg/ml aprotinin, 10 μg/ml leupeptin. The cell lysates were clarified by centrifugation and 1.3-1.7 mg of total protein was incubated overnight at 4°C with appropriate antibodies and protein A/G PLUS-agarose. The immunoprecipitates were subjected to 7.5% SDS-PAGE, and proteins were transferred to PVDF western blotting membrane (Roche Diagnostics GmbH, Mannheim, Germany). Membranes were probed with appropriate antibodies followed by incubation with horseradish peroxidase-conjugated secondary antibodies. The immune complexes were visualized by an enhanced chemiluminescence detection system.

FACS analysis

MCs unstimulated or stimulated with 20 nM uPA for 20 hours were detached from culture plates with 10 mM EDTA, washed with ice-cold PBS, and stained with a murine monoclonal FITC-conjugated anti-C5a receptor antibody that recognized the extracellular peptide corresponding to residues 1-31 (clone W17/1; Serotec Ltd, Oxford, UK), or a FITC-conjugated isotype matched control antibody (Serotec Ltd, Oxford, UK). FACS analysis was performed with a FACScan instrument (Becton-Dickinson).

Immunofluorescence microscopy

Phospho-Stat3 was detected using polyclonal anti-phospho-Stat3 (Tyr705) antibody (Cell Signaling Technology (Beverly, MA, dilution 1:1000) and Alexa Fluor 488-conjugated goat anti-rabbit antibody (Molecular Probes, Inc., dilution 1:150). For C5aR immunofluorescent staining, cells were incubated for 2 hours at room temperature with polyclonal anti-human C5aR antibody (Santa Cruz Biotechnology, dilution 1:40) and Alexa Fluor 488-conjugated donkey anti-goat secondary antibody (Molecular Probes, Inc., dilution 1:150). Confocal microscopy studies were performed as previously described (Dumler et al., 1998).

Animals

Male *uPAR*$^{-/-}$ mice on a mixed C57BL/6J (75%) × 129 (25%) background and their wild-type littermate controls were kindly provided by P. Carmeliet and M. Dewerchin (Leuven, Belgium) and were further bred under the same pathogen-free conditions in the animal facility of Hanover Medical School. All mice, weighing 25-30 g, were used at 8-12 weeks of age. Experiments were conducted in accordance to the regulations of the local authorities.

LPS-induced nephritis

Mice were injected intraperitoneally with either 50 μg LPS (2.0 mg/kg; *Escherichia coli* serotype O111:B4; Sigma Chemical Co, St Louis, MO, USA) in 200 μl of saline or with saline vehicle alone. At 8 hours after injection, the mice were killed and immediately perfused for 10 minutes through the left ventricle into the opened vena cava at an approximate rate of 1 ml/minute of cold PBS. Perfusion quality was optically controlled by observing the organ color change. Large perfusion volumes were used to remove contaminating C5aR-expressing leukocytes from the blood vessels. The kidneys were then harvested, sectioned, the medulla was removed and pieces of kidney cortex containing predominantly glomeruli were snap frozen for RT-PCR experiments and immunohistochemical staining.

Quantitative RT-PCR analysis of uPA, uPAR, C5aR and MCP-1 expression in mouse kidney cortex

Total RNA was isolated from kidney cortex using the RNeasy Mini Kit (QIAGEN GmbH, Germany) and real-time quantitative RT-PCR for uPA, uPAR, C5aR, and MCP-1 serving as a marker of LPS-induced inflammation was performed on a TaqMan ABI 7700 Sequence Detection System (Applied Biosystems, Foster City, CA). β-tubulin was used as a reference gene. The following oligonucleotide primers and probes were used: β-tubulin, 5′-CACCATGAGCGGCGTCA-3′ (sense), 5′-TTCGAAGGTCAGCATTAAGCTG-3′ (antisense), 6-FAM-ACCTGCCTCCGTTTCCCGGG-TAMRA (probe); MCP-1, 5′-CCAACTCTCACTGAAGCCAGC-3′ (sense), 5′-CAGGCCCAGAAGCATGACA-3′ (antisense) 6-FAM-CTCTCTTCCTCCACCACCATGCAGGT-TAMRA (probe); uPA, 5′-CGATTCTGGAGGACCGCTTA-3′ (sense), 5′-CCAGCTCACAATCCCACTCA-3′ (antisense), 6-FAM-CTGTAACATCGAAGGCCGCCCAACT-TAMRA (probe); uPAR, 5′-CCACAGCGAAAAGACCAACA-3′ (sense), 5′-CGGTCTCTGTCAGGCTGATGA-3′ (antisense), 6-FAM-ATGAGTTACCGCATGGGCTCCA-TAMRA (probe); C5aR, 5′-TGTGGGTGACAGCCTTCGA-3′ (sense), 5′-CCGCCAGATTCAGAAACCAG-3′ (antisense), 6-FAM-CCAGACGGGCCGTCAAACGC-TAMRA (probe).

Immunohistochemical studies

The cryosections (6 μm) were fixed with ice-cold acetone and air-dried. Non-specific binding sites were blocked with 10% normal donkey serum (Jackson Immuno Research Lab, West Grove, USA) for 30 minutes. Then sections were incubated with the monoclonal rat anti-mouse C5aR antibody for 1 hour. For fluorescent visualization of bound primary antibodies, sections were further incubated with Cy3-conjugated secondary donkey anti-rat antibody (Jackson Immune Research Lab, West Grove, USA) for 1 hour. Specimens were analyzed using a Zeiss Axioplan-2 imaging microscope with the digital image-processing program AxioVision 3.0 (Zeiss, Jena, Germany). C5aR expression in the glomeruli was evaluated in a blind fashion in arbitrary units (0-5+) based on the staining intensity and positivity of the mesangium using the following criteria: 5+: >90% positive glomeruli with strong immunoreactivity; 4+: >75% positive glomeruli with strong immunoreactivity; 3+: >75% positive glomeruli with weak immunoreactivity; 2+: >25% positive glomeruli with weak immunoreactivity; 1+: >10% positive glomeruli with weak immunoreactivity. Fifteen different cortical areas of each kidney (n=6 for each group) were analyzed.

Statistical analysis

All values are expressed as the mean ± s.e.m. To analyze differences in mean values the two-sided unpaired Student's t-test was used; $P<0.05$ was considered significant, and $P<0.01$ was considered highly significant.

Results

uPA upregulates expression of C5aR in MCs

We began by examining the ability of uPA to regulate expression of C5aR in normal human mesangial cells. The changes in C5aR expression were monitored at the mRNA and protein levels using TaqMan analysis and immunoblotting, respectively. Treatment of MCs with physiological

concentrations of uPA resulted in dramatic increase (up to sevenfold) in C5aR mRNA. This activation was time-dependent and reversible, starting as early as 4 hours, peaking at 16 hours, and returned to basal level at 48 hours (Fig. 1A). Consistent with these data, C5aR protein expression was also upregulated, as shown by immunoblotting using specific anti-C5aR antibody (Fig. 1B). Additionally, we performed FACS analysis and immunocytochemical studies to visualize and quantify C5aR on the cell surface. Indeed, treatment of MCs with uPA led to substantial expression of C5aR on the surface of stimulated cells (Fig. 1C,D). To verify whether uPA exerts its effect on C5aR activation via uPAR, specific uPAR-blocking antibody was used for cell pretreatment. Neither C5aR mRNA nor C5aR protein was upregulated in response to uPA after uPAR blockage (Fig. 2). These data suggest a requirement for uPAR in the chain of signaling events mediating uPA-induced C5aR expression.

uPA potentiates C5aR-related responses in MCs

Since C5aR activation in MCs was shown to induce proliferation and selective production of cytokines and growth factors, we tested whether these functional C5aR-directed responses might be affected by uPA. MCs were stimulated with uPA and C5a separately and simultaneously, and then cell proliferation and production of MCP-1 were analyzed (Fig. 3). In both cases stimuli worked synergistically when added together. These data provide evidence that uPA functions as a modulator of the C5aR-dependent processes in human MCs. To verify the role of uPAR in the observed effects, MCs were pretreated with uPAR blocking antibody. This antibody, in contrast to non-relevant IgG, abolished synergistic effects of uPA and C5a for both MC proliferation and MCP-1 release (Fig. 3).

uPA induces activation of Stat3 and Tyk2 in MCs

Next, we investigated the molecular mechanisms underlying the revealed uPA-induced expression of C5aR. As no data on signaling pathways mediating C5aR expression are available, we asked whether the signal transducer and activator of transcription Stat3 might be one likely candidate. This transcription factor was recently shown to regulate expression of another G-protein-coupled receptor (Senga et al., 2003). To test this hypothesis, we first checked whether uPA could activate Stat3 in MCs. Indeed, stimulation with uPA caused a significant increase in Stat3 tyrosine phosphorylation, as shown in immunoblotting experiments using an antibody that specifically recognized Stat3 phosphorylation on Tyr 705 (Fig. 4A). Stat3 activation was time-dependent and reversible, peaking after 20 minutes of uPA stimulation. This activation was specific for Stat3, as no changes in phosphorylation state of other Stat proteins, namely Stat1, Stat2, Stat4 and Stat5 were observed (data not shown). To determine whether uPA-induced activation of Stat3 results in its translocation to the cell nucleus as required for the functional effect

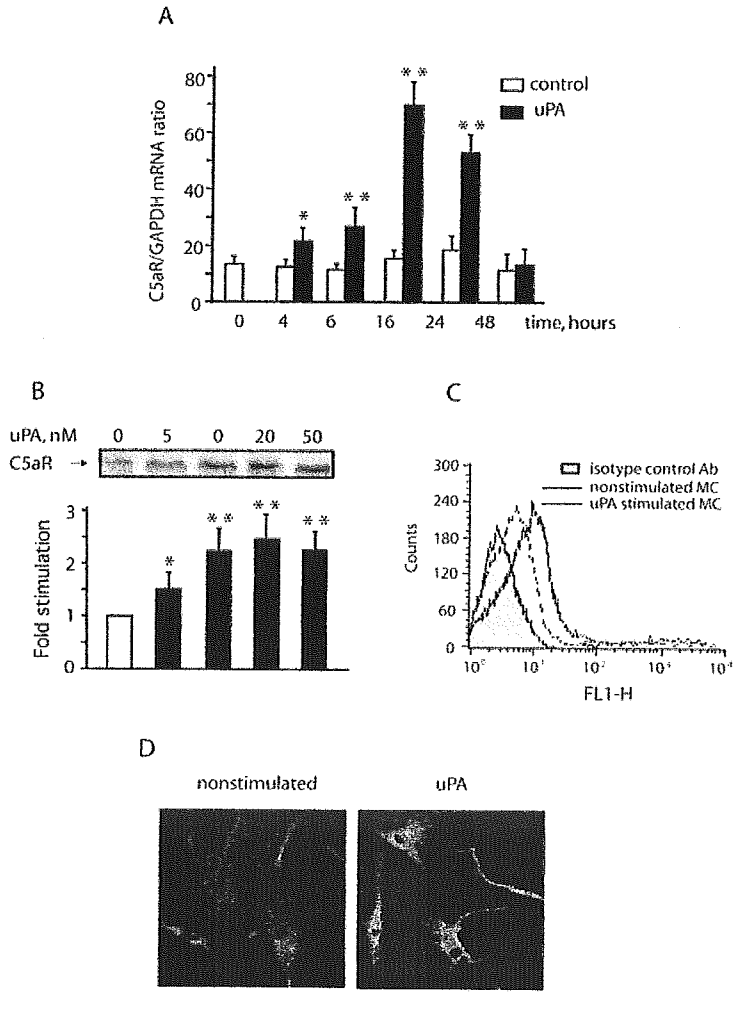

Fig. 1. uPA upregulates expression of C5aR in MCs. (A) RT-PCR analysis for C5aR mRNA was performed using the TaqMan method. RNA was isolated from quiescent MCs incubated for the indicated times with 20 nM uPA or in medium without uPA (control). *GAPDH* served as a house keeping gene. The results are presented as mean ± s.e.m. of four separate and independent experiments. (B) The quiescent MCs were stimulated for 20 hours at 37°C with the indicated concentrations of uPA, and C5aR protein was visualized in the membrane fractions by immunoblotting with anti-C5aR antibodies. MCs incubated in medium without uPA served as a control. The data on the upper panel are representative of four separate and independent experiments. Quantification of the results of these experiments by densitometry presented as mean ± s.e.m. is shown in the lower panel. Significance between control unstimulated and stimulated cells was determined by Student's *t*-test (**P*<0.05; ***P*<0.01). (C) FACS analysis of MCs stimulated (solid line) or not (dashed line) for 20 hours at 37°C with 20 nM uPA using a FITS-labeled murine monoclonal anti-C5aR antibody. FITS-labeled isotype-matched antibody was used as a negative control (grey area). The results are representative of two separate and independent experiments. (D) The quiescent MCs were stimulated for 20 hours with 20 nM uPA or in medium without uPA (control). The cells were then fixed and stained with primary anti-C5aR antibodies and Alexa Fluor 488-conjugated secondary antibodies. Results are representative of three separate experiments.

Journal of Cell Science